

# Hybrid Endometrial-Derived Hydrogels: Human Organoid Culture Models and In Vivo Perspectives

María Gómez-Álvarez, Clara Bueno-Fernandez, Adolfo Rodríguez-Eguren, Emilio Francés-Herrero, Marcos Agustina-Hernández, Amparo Faus, Fernando Gisbert Roca, Cristina Martínez-Ramos, Amparo Galán, Antonio Pellicer, Hortensia Ferrero,\* and Irene Cervelló\*

The endometrium plays a vital role in fertility, providing a receptive environment for embryo implantation and development. Understanding the endometrial physiology is essential for developing new strategies to improve reproductive healthcare. Human endometrial organoids (hEOs) are emerging as powerful models for translational research and personalized medicine. However, most hEOs are cultured in a 3D microenvironment that significantly differs from the human endometrium, limiting their applicability in bioengineering. This study presents a hybrid endometrial-derived hydrogel that combines the rigidity of PuraMatrix (PM) with the natural scaffold components and interactions of a porcine decellularized endometrial extracellular matrix (EndoECM) hydrogel. This hydrogel provides outstanding support for hEO culture, enhances hEO differentiation efficiency due to its biochemical similarity with the native tissue, exhibits superior in vivo stability, and demonstrates xenogeneic biocompatibility in mice over a 2-week period. Taken together, these attributes position this hybrid endometrial-derived hydrogel as a promising biomaterial for regenerative treatments in reproductive medicine.

## 1. Introduction

The human endometrium, a specialized and highly regenerative tissue lining the uterus, undergoes cyclic changes in response to hormonal fluctuations during each menstrual cycle.<sup>[1]</sup> Comprising the functional and basal layers, the endometrium plays a vital role in fertility by providing a receptive environment for embryo implantation. Estrogen and progesterone regulate endometrial structure and function, orchestrating angiogenesis, decidualization, and immune modulation, among other events.<sup>[2]</sup> As disruptions or alterations in this tissue can lead to reproductive disorders including infertility or pregnancy complications, a healthy endometrium is crucial for achieving and maintaining pregnancy.<sup>[1]</sup> Understanding and mimicking the complex physiology and molecular mechanisms underlying

M. Gómez-Álvarez, C. Bueno-Fernandez, A. Rodríguez-Eguren, E. Francés-Herrero, M. Agustina-Hernández, A. Faus, H. Ferrero, I. Cervelló  
IVIRMA Global Research Alliance  
IVI Foundation  
Instituto de Investigación Sanitaria La Fe (IIS La Fe)  
Valencia 46026, Spain  
E-mail: hortensia.ferrero@ivirma.com; irene\_cervello@iislafe.es  
C. Bueno-Fernandez, E. Francés-Herrero  
Universitat de València  
Department of Pediatrics  
Obstetrics and Gynaecology  
Valencia 46010, Spain


F. Gisbert Roca, C. Martínez-Ramos  
Universitat Politècnica de València  
Centre for Biomaterials and Tissue Engineering  
Valencia 46022, Spain

C. Martínez-Ramos  
Unitat Predepartamental de Medicina  
Universitat Jaume I  
Castellón de la Plana 12071, Spain

A. Galán  
Laboratory of Neuroendocrinology  
Prince Felipe Research Center (CIPF)  
Valencia 46012, Spain

A. Galán  
CIBER de Diabetes y Enfermedades Metabólicas Asociadas (CIBERDEM)  
Instituto de Salud Carlos III  
Madrid 28029, Spain

A. Pellicer  
IVIRMA Global Research Alliance  
IVIRMA  
Rome, Roma 00197, Italy

 The ORCID identification number(s) for the author(s) of this article can be found under <https://doi.org/10.1002/adhm.202303838>

© 2023 The Authors. Advanced Healthcare Materials published by Wiley-VCH GmbH. This is an open access article under the terms of the Creative Commons Attribution-NonCommercial-NoDerivs License, which permits use and distribution in any medium, provided the original work is properly cited, the use is non-commercial and no modifications or adaptations are made.

DOI: 10.1002/adhm.202303838

endometrial function will be essential for managing and personalizing reproductive healthcare. Various animal models, including murine models of Asherman's Syndrome,<sup>[3,5]</sup> have been created to investigate and develop innovative therapeutic approaches for endometrial pathologies. However, these models do not imitate the full complexity of the native human endometrial milieu. To meet the urgent need for advanced cell-based bioengineering strategies, hEOs have emerged as powerful tools for studying the endometrium and associated reproductive disorders.<sup>[6]</sup> Organoids are 3D cell-based models that mimic the structure and function of their corresponding *in vivo* tissue.<sup>[7,8]</sup> In particular, hEOs can reliably reproduce multiple phenotypes of the native human endometrium, providing opportunities for personalized medicine and exploring various aspects of its pathophysiology, including alterations to hormone regulation, response to environmental cues, differentiation to secretory and gestational states, and embryo implantation.<sup>[9,10]</sup>

Another key feature of organoids is their capacity for 3D growth in distinct biomaterials, including synthetic matrices,<sup>[11,12]</sup> natural hydrogels,<sup>[13,14]</sup> or a combination of both (i.e., hybrid hydrogels).<sup>[13,15,16]</sup> The most popular natural hydrogel to culture hEOs is Matrigel (Corning Matrigel Matrix), derived from the basement membrane of the extracellular matrix (ECM) extracted from mouse sarcoma tumors. However, Matrigel has several disadvantages due to its tumorigenic origin, commercial batch-to-batch variations, high cost, and risks for translation into clinical practice, in addition to limited stiffness and poor rheological properties.<sup>[17]</sup> Alternatively, natural hydrogels derived from decellularized tissues and organs provide niche-specific microenvironments by preserving inherent molecules such as growth factors, bioactive peptides and proteins,<sup>[18]</sup> but also have limited stiffness and poor rheological properties.<sup>[19]</sup> Hybrid hydrogels overcome the physical limitations of natural matrices<sup>[7]</sup> by balancing the tissue-specific properties of natural hydrogels with the custom-engineered profiles of synthetic hydrogels.<sup>[20]</sup>

Hybrid hydrogels generally comprise synthetic and natural hydrogel components in a well-balanced ratio.<sup>[20]</sup> Multiple bioengineering studies employed RADA<sub>16</sub>, commercialized as PM (Corning), as the synthetic component.<sup>[21,22]</sup> The PM peptide hydrogels consist of 1% standard amino acids – arginine (R), alanine (A), and aspartic acid (D) – and 99% water. Under physiological conditions, the peptides self-assemble into a hydrogel with a nanometer-scale fibrous structure.<sup>[23]</sup> PM applications not only include *in vitro* spheroid cultures,<sup>[24,25]</sup> but also *in vivo* treatments for hemostasis in cardiovascular, gastrointestinal, and otorhinolaryngological surgical procedures in humans.<sup>[26]</sup> Interestingly, the FDA approved a 2.5% RADA<sub>16</sub> formulation for clinical use in 2019,<sup>[27]</sup> positioning PM-based hydrogels as an attractive biomaterial for translational studies. Regarding the natural components of hybrid hydrogels, tissue-specific ECM hydrogels are gaining traction due to their unique biochemical composition and native biological properties.<sup>[28]</sup> The ECM is a 3D network of macromolecules that provides structural support for the cells while orchestrating cell signaling, functions, and properties.<sup>[29]</sup> ECM hydrogels are derived

from decellularized organs or tissues, through enzymatic and/or physical processes that remove cellular components while preserving the integrity of the ECM.<sup>[30]</sup> Remarkably, decellularization techniques generate tissue-specific and immunotolerant biomaterials that can be used for a broad range of clinical applications.<sup>[31]</sup> Decellularized tissues are then solubilized and neutralized to create a pre-gel form that can be used *in vitro* and *in vivo*.<sup>[31]</sup> ECM hydrogels are promising scaffolds for regenerative medicine because they promote cell growth, migration, function, differentiation, angiogenesis, antimicrobial effects, niche responses, mechanical support, and chemotactic effects.<sup>[29,32]</sup> Alternatively, synthetic hydrogels can be mass-produced with precise control over the molecular weight, architecture, and microscopic morphology. Their mechanical properties can easily be tailored to improve the strength, stability, and degradability for a given application.<sup>[33]</sup> The problem remains that most synthetic components only function as passive support and do not promote active and tissular/organ specific cellular interactions. The addition of natural hydrogels overcomes this limitation, not only by imitating the native milieu but also by promoting biological activities, hierarchical organization, and structural integrity that uphold *in vitro* and *in vivo* uses in tissue engineering.<sup>[34]</sup> Further, the natural protein scaffolding and bioactive factors induce a more realistic activation of cellular responses, differentiation processes, and cell-triggered remodeling.<sup>[18]</sup>

Natural ECM derived from decellularized endometrium hydrogels significantly improved *in vitro* cell culture with the ability to mimic the native milieu of the uterus.<sup>[35,36]</sup> EndoECM hydrogels derived from different species, such as the pig,<sup>[35,37]</sup> cow,<sup>[28]</sup> and human<sup>[28,38]</sup> have been characterized. In terms of applications, porcine EndoECM hydrogels were supplemented into hEO culture medium<sup>[39]</sup> while bovine and human EndoECM hydrogels were successfully applied as 3D scaffolds.<sup>[28]</sup> However, these studies presented undifferentiated hEO models and did not evaluate the temporal behavior of EndoECM hydrogels *in vivo*. Nevertheless, intrauterine porcine EndoECM hydrogel treatment regenerated endometrial tissue and enhanced fertility in animal models of uterine damage.<sup>[36]</sup> Taken together, these *in vitro* and *in vivo* advances provide foundational studies for translating EndoECM-based therapies to patients with uterine-factor infertility.

We present a hybrid endometrial-derived hydrogel that combines PM and porcine EndoECM hydrogel (50:50), thoroughly characterized by rheology, scanning electron microscopy (SEM), and proteomic analysis. We demonstrated the suitability of this hybrid endometrial-derived hydrogel to support the 3D growth of hEOs by evaluating viability, morphology, proliferation, and differentiation. To determine whether the hybrid endometrial-derived hydrogel promoted the differentiation of hEOs into the secretory and gestational phases, we assessed SPP1 protein secretion and gene expression of *SPP1*, *PAEP*, *LIF*, *17HSDβ2*, and *SOX9*. Finally, we verified the biocompatibility and *in vivo* dynamics of the hybrid endometrial-derived hydrogel in an immunocompetent murine model, to provide evidence of its safety for future clinical applications.

## 2. Results

### 2.1. Characterization of Hybrid Endometrial-Derived Hydrogel

#### 2.1.1. Rheological Similarities of the Hybrid Endometrial-Derived Hydrogel Based on PM + EndoECM (50:50) and Native Endometrial Tissue

To assess the mechanical properties of the samples, rheological measurements were performed with a parallel-plate rheometer. The storage modulus represents the elastic behavior of the material when deformed (quantifying the recoverable energy in a cycle), while the loss modulus reflects the viscous behavior of the material when deformed (measuring the non-recoverable energy in a cycle due to different dissipative processes). The temporal evolution of the storage and loss modulus were obtained by subjecting samples to a strain of 1% and a frequency of 1 Hz at physiological temperature (37 °C). PM and PM + EndoECM hydrogel (50:50) samples, denoted as the hybrid endometrial-derived hydrogel hereafter, exhibited higher storage and loss moduli compared to the other hybrid hydrogel compositions, with values similar to the native porcine endometrial tissue (**Figure 1A**). This indicated superior viscoelasticity and stronger mechanical strength than the other conditions, including Matrigel + EndoECM hydrogel (50:50), PM + EndoECM hydrogel (25:75), EndoECM hydrogel, and Matrigel.

To determine whether these hydrogels have mechanical properties equivalent to porcine endometrial tissue, we examined the storage modulus (strain = 1%; frequency = 1 Hz), the complex viscosity (strain = 1%; frequency = 1 Hz) and the oscillation stress (shear rate = 10 s<sup>-1</sup>) (**Figure 1A**). All samples exhibited equivalent elastic behavior, as there were no statistical differences in the storage modules between the PM hydrogel, the hybrid endometrial-derived hydrogel, and the control tissue. Similarly, regarding the complex viscosity, no difference was observed between the PM hydrogel, the hybrid endometrial-derived hydrogel, and the native tissue. Therefore, the three samples had an equivalent total resistance to flow when force is applied. Finally, the oscillation stress tests indicated that the strength of the hydrogel networks was equivalent to that of the porcine endometrial tissue. Consequently, we confirm that both PM and hybrid endometrial-derived hydrogel samples had mechanical properties reflecting those of the native endometrium. These results corroborate the notion that these two hydrogels may serve as a more natural and supportive environment for both in vitro and in vivo applications.

#### 2.1.2. Hybrid fiber Combinations Improve Physical and Cellular Support

The ultrastructure of the EndoECM, PM, and hybrid endometrial-derived hydrogels was assessed by SEM. The EndoECM hydrogel showed intricate and homogeneous networks composed of collagen fibers, the principal components of the ECM. The PM hydrogel was composed of a repetitive sequence of RADA<sub>16</sub> peptides, which self-assembled into a  $\beta$ -sheet nanometer-scale fibrous structure with irregularly sized pores<sup>[40]</sup> (**Figure 1B**). The hybrid endometrial-derived hydrogel presented both collagen fibers and RADA<sub>16</sub> peptides with similar morphology and size to EndoECM hydrogel and PM

filaments, respectively. To confirm whether this correspondence was fortuitous or not, fiber diameters were analyzed from  $\times 50\,000$  magnification images and compared between groups according to the type of fiber they presented (EndoECM hydrogel versus hybrid endometrial-derived hydrogel; PM versus hybrid endometrial-derived hydrogel). The average diameter of collagen fibers was  $88.40 \pm 8.91$  nm in the EndoECM hydrogel and  $80.70 \pm 6.60$  nm in the hybrid endometrial-derived hydrogels. Conversely, the average diameter of RADA<sub>16</sub> peptides was  $35.70 \pm 3.90$  nm in the PM and  $33.70 \pm 4.63$  nm in the hybrid endometrial-derived hydrogels. No significant differences between conditions were found, demonstrating that the addition of PM did not perturb the morphology of the hybrid endometrial-derived hydrogel. The presence of both types of components, collagen fibers (from EndoECM hydrogel) and RADA<sub>16</sub> peptides (from PM), in the hybrid endometrial-derived hydrogel was also corroborated. Interestingly, PM nanopeptides created a 3D structure that filled the “gaps” between the collagen fibers in the EndoECM hydrogel, increasing the surface area of the hybrid endometrial-derived hydrogel, and ultimately, its physical support and cell adhesion, as observed in other studies.<sup>[41,42]</sup>

#### 2.1.3. The Hybrid Endometrial-Derived Hydrogel Retains the Native, Endometrial-Specific Matrisomal Profile

The matrisome is defined as the comprehensive ensemble of ECM constituents and functions.<sup>[43]</sup> To evaluate if the addition of PM affects the EndoECM hydrogel matrisome, we quantified the peptides from the EndoECM (Table S1, Supporting Information) and the hybrid endometrial-derived hydrogels (Table S2, Supporting Information) by liquid chromatography and tandem mass spectrometry (LC-MS/MS). The hybrid endometrial-derived hydrogel samples were precipitated to separate the RADA<sub>16</sub> peptides corresponding to the PM and exclusively analyze the matrisomal proteins of the EndoECM hydrogel. The LC-MS/MS analysis revealed 119 and 91 parent proteins in EndoECM and hybrid endometrial-derived hydrogels, respectively. According to the information in the Matrisome database, these proteins were then classified into core matrisome proteins (collagens, ECM glycoproteins, and proteoglycans) and matrisome-associated proteins (ECM regulators, ECM affiliated proteins, and secreted factors). Proteins that were not found in the Matrisome database but located in the extracellular space were grouped into the “other components” category (**Figure 2A**).

Most of the components of the EndoECM hydrogel were retained in the hybrid endometrial-derived hydrogel (**Figure 2A**), suggesting the presence of PM did not perturb the biochemical composition of the EndoECM hydrogel. Among the 33 common proteins between the two protein profiles, we identified the most prominent structural components of the endometrial ECM (collagen types I-III, V, VI, XIV, XXVIII), several glycoproteins (including dermatopontin, Von Willebrand factor, laminin, and elastin), and other ECM-associated proteins (including annexin, elastase, and protein S100) (**Figure 2B,C**). The six proteins not maintained in the hybrid endometrial-derived hydrogel were fibrinogen gamma chain (FGG), collagen type 4 alpha 1 and 2 (COL4A1, COL4A2), collagen type 5 alpha 3 (COL5A3), serpin

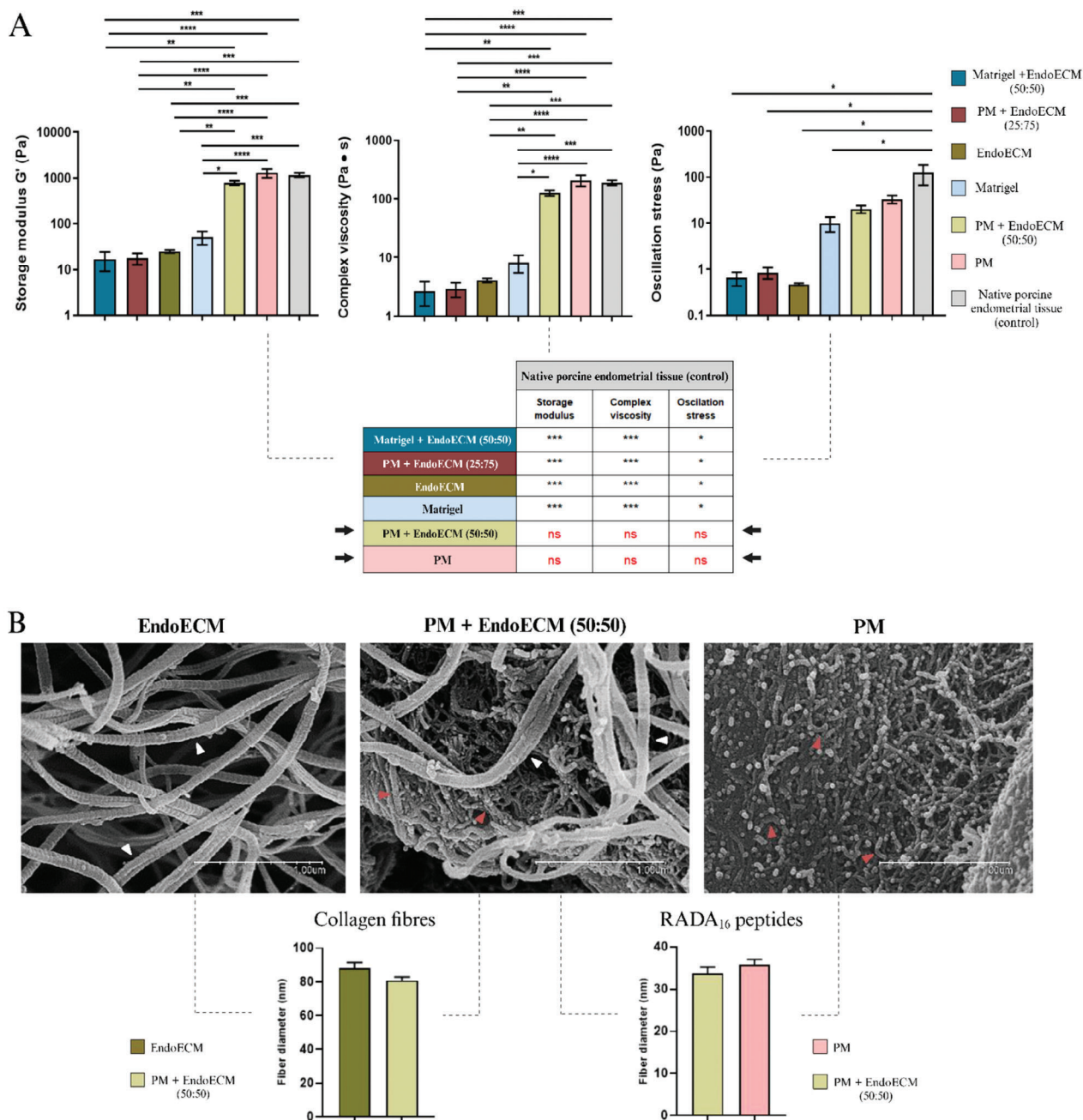


**Figure 1.** Rheological analyses and scanning electron microscopy of hydrogels. A) Storage modulus (strain = 1%; frequency = 1 Hz), complex viscosity (strain = 1%; frequency = 1 Hz) and oscillation stress (shear rate =  $10 \text{ s}^{-1}$ ) at  $37^\circ\text{C}$  for EndoECM, Matrigel, PM, PM + EndoECM (50:50) hydrogels, and other hybrid combinations [Matrigel + EndoECM (50:50), PM + EndoECM (25:75)]. The rheological properties of native porcine endometrial tissue (control) are also represented. There were no statistically differences between the rheological properties of PM + EndoECM hydrogel (50:50) and PM samples (black arrows) compared to those of porcine endometrial tissue.  $N = 3$  technical replicates/group. \*\*\*\* $p < 0.0001$ ; \*\*\* $p < 0.001$ ; \*\* $p < 0.01$ ; \* $p < 0.05$ . Notably, PM + EndoECM hydrogel (50:50) was established as the best hybrid endometrial-derived hydrogel and was further evaluated with subsequent analyses. B) Scanning electron microscopy images of EndoECM hydrogel, PM, and PM + EndoECM (50:50) hydrogel at 50.0 k magnification. The diameter of the collagen fibers (white arrows) was compared in EndoECM and PM + EndoECM (50:50) hydrogels; the diameter of the RADA<sub>16</sub> peptides (red arrows) was compared in PM and PM + EndoECM (50:50) hydrogels.  $N = 3$  technical replicates/group. Scale bars =  $1 \mu\text{m}$ .

peptidase inhibitor clade B member 1 (SERPINB1), and S100 calcium binding protein A9 (S100A9) (Figure 2B).

Collectively, the collagen fibers were the most enriched matrisomal components [46.17% in the EndoECM hydrogel (Figure 2A) and 44.30% in the hybrid endometrial-derived hy-

drogel (Figure 2B)], which is likely due to their essential mechanical and structural role in the ECM.<sup>[44]</sup> Similar proportions of ECM glycoproteins were also observed (27.15% in the EndoECM hydrogel and 21.18% in the hybrid endometrial-derived hydrogel) but proteoglycans were absent in all samples. The

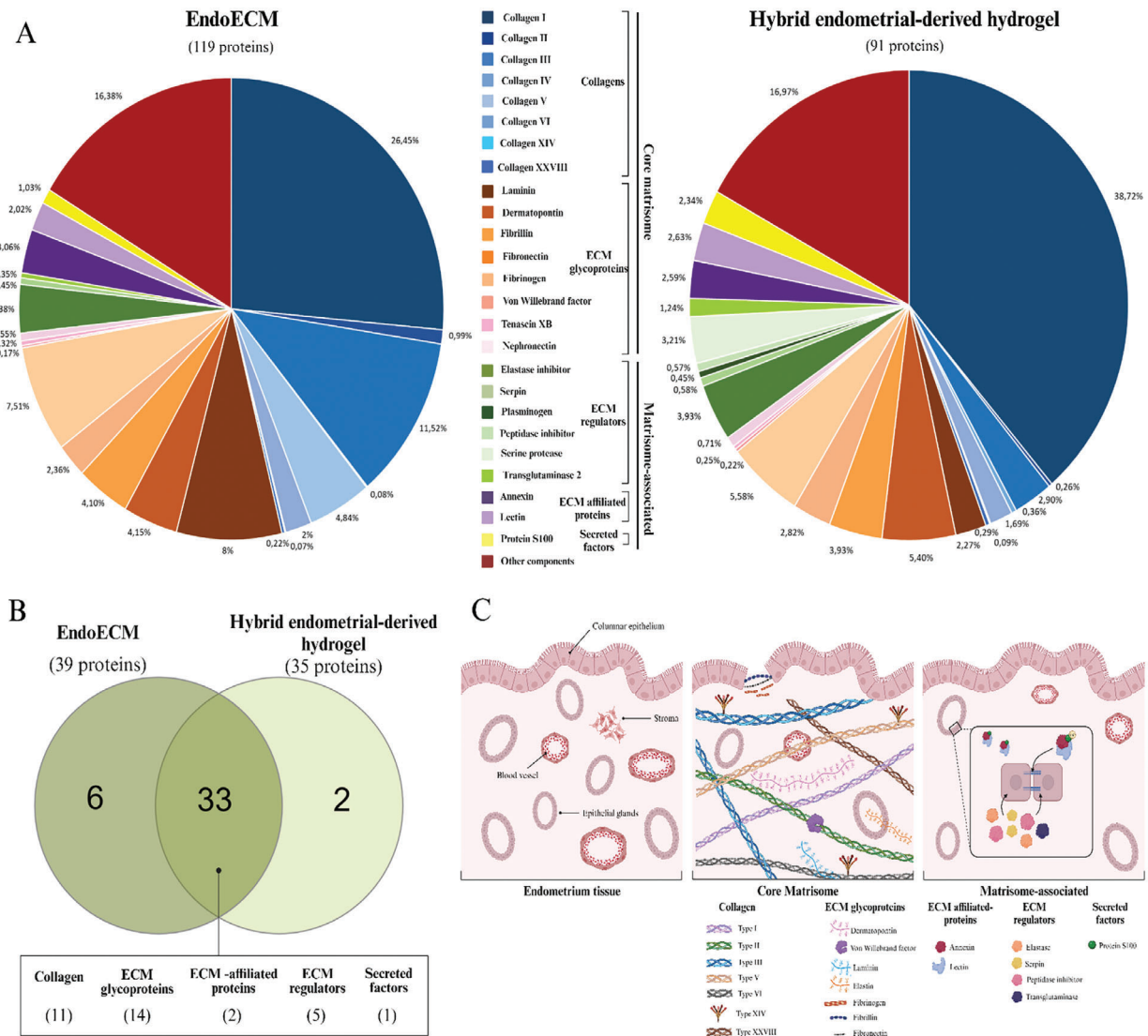


**Figure 2.** Matrisomal protein profile in EndoECM and hybrid endometrial-derived hydrogels. A) The protein profiles for each condition (EndoECM and hybrid endometrial-derived hydrogels), reflecting the proportion of core matrisome and matrisome-associated proteins. B) Venn diagram depicting the relationships of the common matrisomal components in the EndoECM and hybrid endometrial-derived hydrogels. C) Molecular representation of the complexity of the endometrial ECM, highlighting the common matrisomal proteins identified between the EndoECM and the hybrid endometrial-derived hydrogels. Created with BioRender.com.

percentage of matrisome-associated proteins was slightly higher in the hybrid endometrial-derived hydrogel (17.55%) compared to the EndoECM hydrogel (10.30%). The “other components” category represents multiple proteins (16.38% in the EndoECM hydrogel and 16.97% in the hybrid endometrial-derived hydrogel), some of them related to ECM remodeling, like caveolin.<sup>[45]</sup> No immunoreactive molecules and major histocompatibility complex antigens were found. Employing the aforementioned ECM proteins in a functional enrichment analysis with the GO database highlighted several biological processes and molecular functions related to the ECM (Table S3, Supporting Information). Notably, the analysis of the PM fraction from the hybrid endometrial-derived hydrogel revealed the presence of 100% RADA<sub>16</sub> peptides (Table S2, Supporting Information), consistent with the biochemical composition of the PM [99% water and 1% repeated se-

quences of three different amino acids: arginine (R), alanine (A), and aspartate (D)].

Overall, these findings support that the hybrid endometrial-derived hydrogel preserves the matrisomal profile of the native endometrium, corroborating its native origin and contributing to the maintenance of its specific functions.

#### 2.1.4. Comparative Proteomic Analysis of Human, Bovine, and Hybrid Endometrial-Derived Hydrogels: How Functionally Similar are they to the Native Human Endometrium?

To assess how the protein composition of the hybrid endometrial-derived hydrogel relates to those of previously described hydrogels, we compared the proteomic results with those from

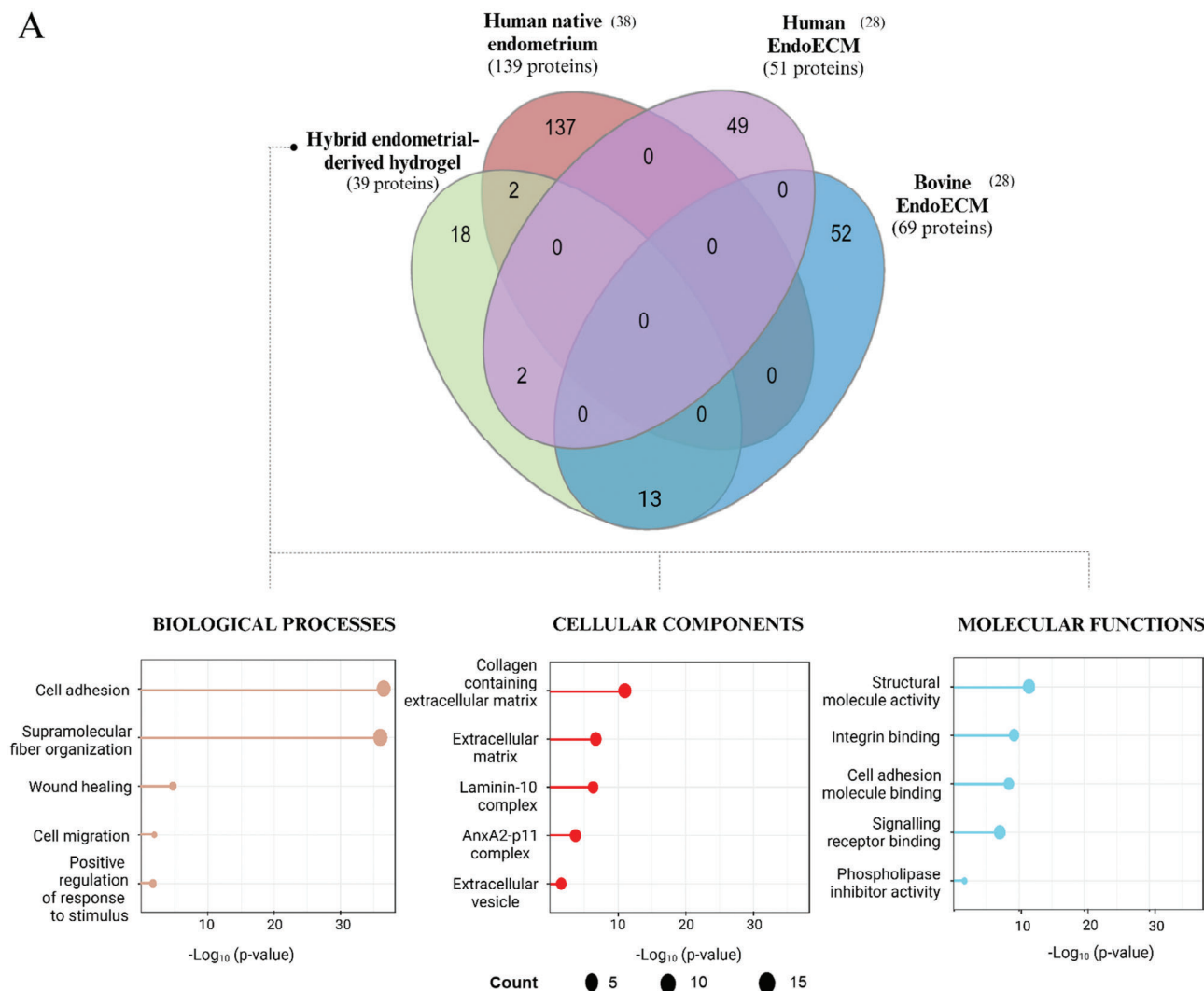


**Figure 3.** Proteomic comparison between the hybrid endometrial-derived hydrogel, the bovine EndoECM hydrogel, the human EndoECM hydrogel, and the native human endometrium. A) (Above) Venn diagram highlighting the relationships of the proteins identified in the three hydrogels and the native human endometrium. (Below) The significant biological processes, cellular components, and molecular functions shared between the hybrid endometrial-derived hydrogel and the human native endometrium. B) Heatmap depicting the common (green) and different (red) biological processes between the different hydrogels and the human native endometrium. Note: Proteomics data from the bovine EndoECM hydrogel,<sup>[28]</sup> human EndoECM hydrogel,<sup>[38]</sup> and native human endometrium<sup>[38]</sup> were retrieved from previous publications by other research groups.

studies characterizing bovine<sup>[28]</sup> or human EndoECM hydrogels<sup>[38]</sup> and the human native endometrium<sup>[38]</sup> (Figure 3A). Surprisingly, only the hybrid endometrial-derived hydrogel shared two proteins with the human native tissue: annexin II and laminin. Annexin II is essential for embryo adhesiveness to the endometrial tissue<sup>[46]</sup> whereas laminin promotes endometrial epithelial remodeling and embryo implantation during the menstrual cycle.<sup>[47]</sup> Neither the bovine nor human EndoECM hydrogels had any proteins in common with the native human endometrial tissue. Alternatively, the hybrid endometrial-derived hydrogel shared 13 and 2 proteins with the bovine and human EndoECM hydrogels, respectively. Interestingly, the human and bovine EndoECM hydrogels did not have any common proteins.

We also showed the significantly enriched biological processes, cellular components, and molecular functions shared be-

tween the hybrid endometrial-derived hydrogel and the human native endometrium. To achieve this, a functional enrichment analysis was conducted on the proteins present in each condition, followed by a comparison and representation of the most significant common biological processes, cellular components, and molecular functions (Figure 3A). The most significantly enriched biological processes included fiber organization, cell adhesion and migration, and positive response to stimulus, which are all essential for in vitro cell culture. As expected, the proteins were mainly located in the ECM as part of the collagen, laminin, and annexin complexes. Of note, the most relevant molecular functions were related to structural molecule activity, cell adhesion molecule binding, and signaling receptor binding. Remarkably, comparison of the enriched biological processes between all hydrogels and with the human native endometrium revealed the

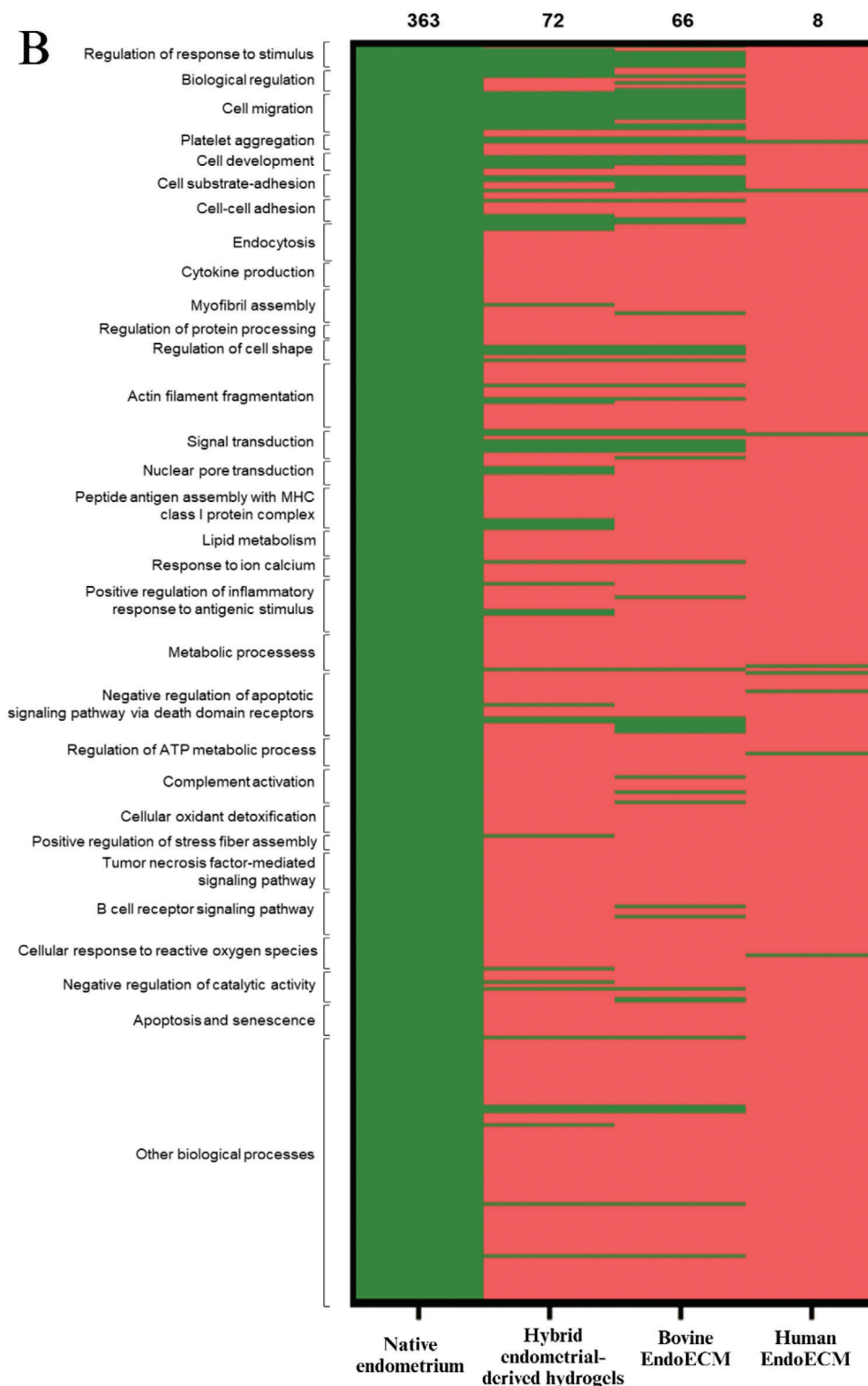


Figure 3. Continued

hybrid endometrial-derived hydrogel shared the most biological processes with the human native endometrial tissue (72 out of 363), followed by the bovine EndoECM (66 out of 363) and the human EndoECM (8 out of 363) hydrogels (Figure 3B). These re-

sults distinguish the similarity between the hybrid endometrial-derived hydrogel and the human native tissue, providing evidence the hybrid endometrial-derived hydrogel is superior to other reported hydrogels.

## 2.2. Biological Applications of the Hybrid Endometrial-Derived Hydrogel

### 2.2.1. Support *in vitro* Culture and 3D Development of hEOs

Rheological analyses revealed that PM and the hybrid endometrial-derived hydrogels possessed mechanical properties resembling the native endometrial tissue, therefore we evaluated their suitability for *in vitro* patient-derived organoid culture. We cultured hEOs in Matrigel ( $n = 4$ ) as previously described.<sup>[6]</sup> After one passage, hEOs were collected and seeded in a 96-well culture plate, utilizing either the hybrid endometrial-derived or PM hydrogels (for the experimental conditions) or Matrigel (control condition) as 3D support. After 7 days of culture, there were no organoids in the PM hydrogel. However, the hybrid endometrial-derived hydrogel was able to maintain the formation, growth, and development of hEOs comparable to Matrigel (Figure 4A). Under bright-field microscopy, the hybrid endometrial-derived hydrogel appeared cloudier and the hEOs cultured within it were darker in appearance when compared to the Matrigel, which may be attributed to the PM consistency. The LIVE/DEAD assay demonstrated there was >98% cell viability in all samples, confirming excellent survival rates of hEOs cultured in the hybrid endometrial-derived hydrogel. While hematoxylin and eosin (H&E) staining of the hEOs revealed they had a similar morphology in the hybrid endometrial-derived hydrogel and Matrigel conditions, Ki67 immunohistochemistry showed a notable increase in cell proliferation in the hybrid endometrial-derived hydrogel. The epithelial origin of the hEOs was confirmed by double immunofluorescence for E-cadherin and vimentin. The strong expression of E-cadherin coupled with the absence of vimentin indicated an enrichment of epithelial cells over stroma in both the hybrid endometrial-derived hydrogel and Matrigel.<sup>[39]</sup> Finally, the expression of laminin was observed in hEOs grown in Matrigel and the hybrid endometrial-derived hydrogel. These findings corroborate the essential role of laminin in organoid development and differentiation, and support how it could improve the organoid forming efficiency.<sup>[17]</sup>

### 2.2.2. Improving hEO Differentiation to Secretory and Gestational Stages

Once the hEO culture was established in the hybrid endometrial-derived hydrogel, we evaluated the ability of this biomaterial to promote the differentiation of the hEOs. Following protocols previously established,<sup>[6]</sup> hEOs were first exposed to estradiol, progesterone, and cyclic adenosine monophosphate to promote the transition to the secretory phase. Then, prolactin and placental lactogen were added to mimic the early gestational stage. Culture media and hEOs were collected for protein secretion and gene expression analyses, respectively.

We evaluated osteopontin (SPP1) secretion from the culture media of hEOs by enzyme-linked immunosorbent assay (ELISA). Under physiological conditions, SPP1 secretion increases in the secretory and gestational endometrium to promote embryo attachment and facilitate trophoblast invasion during embryo implantation.<sup>[48]</sup> Surprisingly, we detected a significant amplification of SPP1 in the culture media of gestational hEOs that were

grown in the hybrid endometrial-derived hydrogel (fold change [FC] =  $1.103 \pm 0.03$ ) compared to all other conditions (Figure 4B).

Next, we evaluated the changes in the gene expression of *SPP1*, *PAEP*, *LIF*, *17HSD $\beta$ 2*, and *SOX9* by quantitative real-time PCR (qRT-PCR). These markers were selected based on their roles in uterine function: *LIF* promotes embryo attachment and trophoblast invasion,<sup>[49]</sup> *PAEP* modulates immune responses and is associated with better pregnancy outcomes,<sup>[50]</sup> and *17HSD $\beta$ 2* locally regulates steroid hormones to maintain an endometrial environment that favors successful embryo implantation and placental development.<sup>[51]</sup> We found a significant upregulation of *SPP1* (Figure 4C), *PAEP* (Figure 4D), *LIF* (Figure 4E), and *17HSD $\beta$ 2* (Figure 4F) in the secretory-stage hEOs grown in hybrid endometrial-derived hydrogel versus Matrigel (FC =  $7.53 \pm 1.79$ ; FC =  $242.5 \pm 187.2$ ; FC =  $4.98 \pm 2.43$ ; FC =  $4.69 \pm 1.03$ , respectively,  $p < 0.05$ ). Undifferentiated hEOs cultured in the hybrid endometrial-derived hydrogel also overexpressed *LIF* and *17HSD $\beta$ 2* (FC =  $3.49 \pm 0.83$  and FC =  $27.60 \pm 10.13$ , respectively) compared to the undifferentiated hEOs cultured in Matrigel. During the gestational phase, only *17HSD $\beta$ 2* was significantly upregulated in hEOs grown in the hybrid endometrial-derived hydrogel (FC =  $7.29 \pm 3.46$ ,  $p < 0.05$ ) compared to the hEOs grown in Matrigel.

In line with the expression of these markers, we found lower expression levels of *SOX9* (Figure 4G) in secretory hEOs grown in the hybrid endometrial-derived hydrogel (FC =  $0.18 \pm 0.06$ ) versus Matrigel. In the context of hEOs, *SOX9* downregulation during differentiation indicates the transition from a progenitor-like state to specialized cell lineages with distinct functions.<sup>[52,53]</sup>

To further demonstrate how the hydrogels support hEO differentiation, we also analyzed the differences in *SPP1* secretion and *SPP1*, *PAEP*, *LIF*, *17HSD $\beta$ 2*, and *SOX9* gene expression between the differentiation stages (undifferentiated, secretory, and gestational) within the Matrigel and hybrid endometrial-derived hydrogel groups (Figure S1, Supporting Information). In the hybrid endometrial-derived hydrogel condition, *SPP1* secretion of secretory and gestational hEOs was statistically higher than undifferentiated hEOs. However, no statistically differences between the *SPP1* secretion of differentiated and undifferentiated hEOs grown in Matrigel were found. Regarding gene expression, we observed higher expression of *SPP1*, *PAEP*, *LIF*, and *17HSD $\beta$ 2* in secretory and gestational hEOs compared to undifferentiated hEOs in both conditions. Interestingly, *SOX9* downregulation was only present in hEOs cultured in the hybrid endometrial-derived hydrogel (Figure S1, Supporting Information). Together, these findings confirmed the suitability of the hybrid endometrial-derived hydrogel to support and improve hEO differentiation.

### 2.2.3. A Stable, Xenogeneic, and Immunotolerated Biomaterial for *In Vivo* Use

The biocompatibility of the hybrid endometrial-derived hydrogel was assessed *in vivo* in an immunocompetent murine model for 14 days. We subcutaneously injected non-decellularized endometrial extracellular matrix hydrogel (Endo-NoDC), PM, and the hybrid endometrial-derived hydrogel in female C57BL/6 mice ( $N = 30$ ). We accounted for the absence of blood



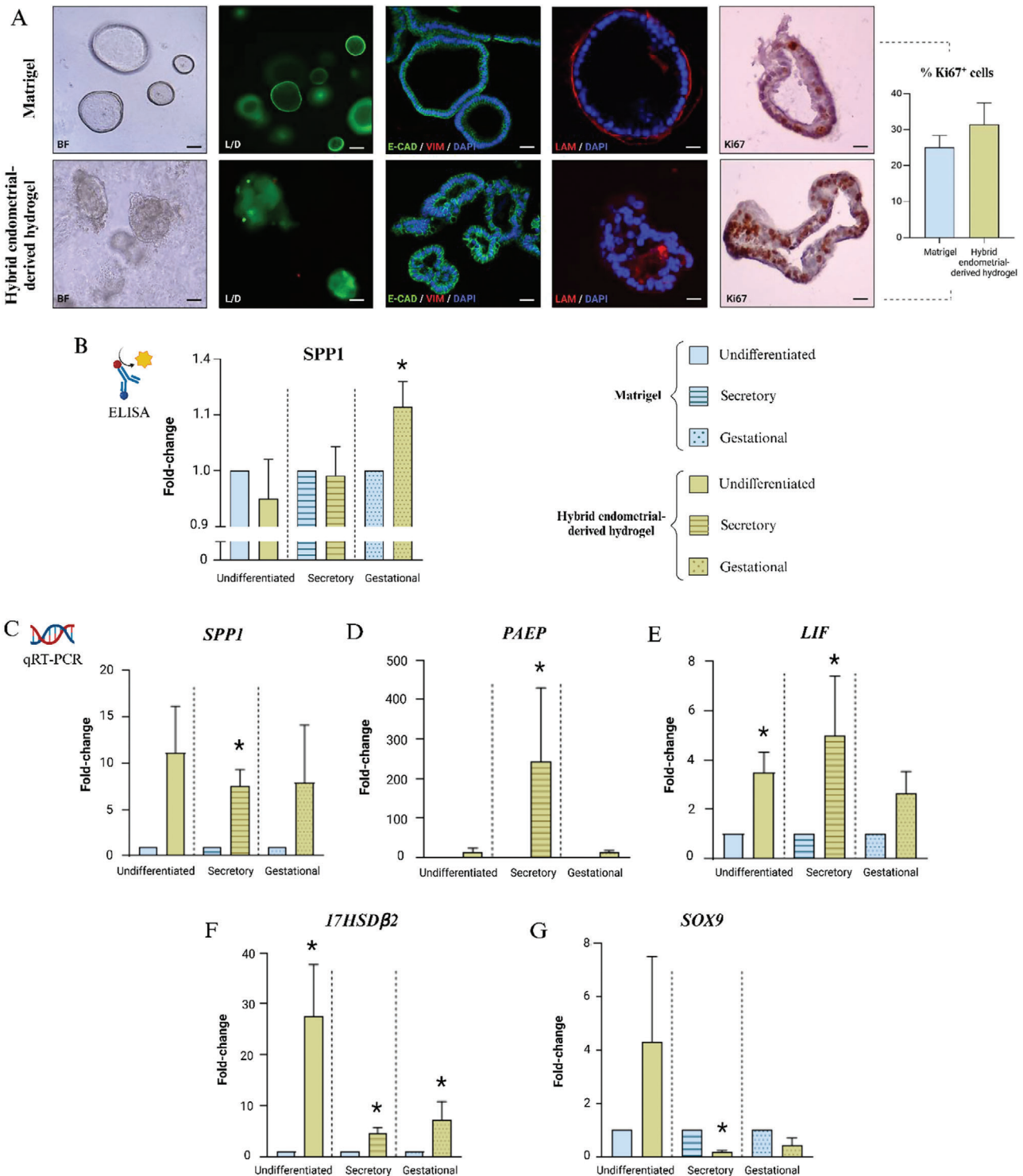


**Figure 4.** Hybrid endometrial-derived hydrogel supports the in vitro culture of undifferentiated hEOs and improves their differentiation to the secretory and gestational phases. A) Representative images of hEOs cultured in the hybrid endometrial-derived hydrogel or Matrigel control captured during (from left to right) bright-field microscopy (BF), LIVE/DEAD assay (L/D), double immunofluorescence for E-cadherin (E-CAD) (green) and vimentin (VIM) (red), single immunofluorescence for laminin (LAM) (red), and immunostaining for Ki67 (Ki67). Scale bars = 50  $\mu$ m. B) Quantification of SPP1 secretion into the culture media of undifferentiated and differentiated hEOs grown in both hydrogels, determined by ELISA. Relative gene expression of C) *SPP1*, D) *PAEP*, E) *LIF*, F) *17HSD $\beta$ 2*, and G) *SOX9* in hEOs cultured in Matrigel or hybrid endometrial-derived hydrogel conditions determined by qRT-PCR analysis. Data are presented as the mean fold change from N = 4 biopsies (calculated with respect to the expression in the paired Matrigel group)  $\pm$  standard error of mean. \* $p < 0.05$ .

**Table 1.** Hematological values obtained from the blood of female C57BL/6 mice treated with Endo-NoDC, PM, and hybrid endometrial-derived hydrogels. Compilation of the proportion of neutrophils (NEUT), lymphocytes (LYMPH), monocytes (MONO), eosinophils (EOS), and basophils (BASO); the red blood cell (RBC), and platelet (PLT) concentrations. Control female C57BL/6 values were obtained from Charles River's Laboratory published data.<sup>[54]</sup> Abnormally low values are highlighted in bold. Data are presented as mean  $\pm$  standard deviation (SD). N = 30 mice (10 mice/condition).

		NEUT [%]	LYMPH [%]	MONO [%]	EOS [%]	BASO [%]	RBC [M $\mu\text{L}^{-1}$ ]	PLT [K $\mu\text{L}^{-1}$ ]	
Control <sup>9</sup> C57BL/6	Mean	14	79.55	4.37	1.69	0.34	9.24	1167	
	95% interval	Low	7.44	70.19	2.18	0.20	0.02	7.37	565
		High	22.67	87.82	7.06	4.51	1.26	11.50	1849
Endo-NoDC	Mean $\pm$ SD (Day 2)	20.30 $\pm$ 9.98	72.73 $\pm$ 9.44	3.27 $\pm$ 1.19	3.40 $\pm$ 1.51	0.30 $\pm$ 0.20	5.80 $\pm$ 3.48	143 $\pm$ 113.21	
	Mean $\pm$ SD (Day 7)	13.83 $\pm$ 2.63	81.00 $\pm$ 3.18	3.43 $\pm$ 0.31	1.47 $\pm$ 0.32	0.17 $\pm$ 0.06	6.84 $\pm$ 1.20	280 $\pm$ 389.20	
	Mean $\pm$ SD (Day 14)	13.45 $\pm$ 5.03	83.00 $\pm$ 5.48	2.18 $\pm$ 0.33	1.15 $\pm$ 0.41	0.23 $\pm$ 0.10	7.91 $\pm$ 0.34	481 $\pm$ 301.01	
PM	Mean $\pm$ SD (Day 2)	16.40 $\pm$ 6.20	78.20 $\pm$ 7.89	2.23 $\pm$ 0.31	2.83 $\pm$ 1.59	0.30 $\pm$ 0.06	8.01 $\pm$ 0.71	790 $\pm$ 163.65	
	Mean $\pm$ SD (Day 7)	13.43 $\pm$ 1.67	82.60 $\pm$ 3.27	1.87 $\pm$ 0.40	1.90 $\pm$ 1.55	0.20 $\pm$ 0.10	7.42 $\pm$ 0.36	348 $\pm$ 110.50	
	Mean $\pm$ SD (Day 14)	13.60 $\pm$ 3.09	82.13 $\pm$ 4.32	2.83 $\pm$ 1.25	1.35 $\pm$ 1.27	0.10 $\pm$ 0.08	7.72 $\pm$ 0.69	588 $\pm$ 222.41	
Hybrid endometrial-derived hydrogel	Mean $\pm$ SD (Day 2)	18.87 $\pm$ 3.27	74.20 $\pm$ 4.19	3.67 $\pm$ 0.35	2.70 $\pm$ 0.46	0.57 $\pm$ 0.15	7.67 $\pm$ 0.17	403 $\pm$ 67.82	
	Mean $\pm$ SD (Day 7)	16.80 $\pm$ 0.70	79.00 $\pm$ 0.61	2.50 $\pm$ 0.46	1.27 $\pm$ 0.61	0.43 $\pm$ 0.06	8.58 $\pm$ 0.35	575 $\pm$ 374.50	
	Mean $\pm$ SD (Day 14)	17.05 $\pm$ 5.50	77.20 $\pm$ 5.98	3.35 $\pm$ 0.95	1.95 $\pm$ 0.60	0.45 $\pm$ 0.64	7.68 $\pm$ 0.62	423 $\pm$ 352.87	

disorders and normal cytokine profiles in plasma by subjecting the mice to hematocrit tests at day 2, 7, and 14 post-injection. The Endo-NoDC animals had fewer erythrocytes at day 2 ( $5.80 \pm 3.48 \text{ M } \mu\text{L}^{-1}$ ) and day 7 ( $6.84 \pm 1.20 \text{ M } \mu\text{L}^{-1}$ ) than control animals ( $7.37 \text{ M } \mu\text{L}^{-1}$ ). Despite 60% of mice injected with hydrogels experiencing a decrease in the number of platelets ( $<565 \text{ K } \mu\text{L}^{-1}$ ) only one mouse treated with the Endo-NoDC hydrogel presented with thrombocytopenia at day 2 ( $143 \pm 113.21 \text{ K } \mu\text{L}^{-1}$ ) and 7 ( $280 \pm 389.20 \text{ K } \mu\text{L}^{-1}$ ). Regarding leukocytes, no differences were found in the proportion of neutrophils, lymphocytes, monocytes, eosinophils, and basophils in mice injected with Endo-NoDC, PM, and hybrid endometrial-derived hydrogels with respect to the normal leukocyte values of female C57BL/6 mice<sup>[54]</sup> (Table 1). As no pathological alterations of white blood cells were detected in any of the three conditions, our findings suggest that the hybrid endometrial-derived hydrogel did not cause any systemic immune disorders in our immunocompetent murine model.

Furthermore, the serological profiles of the treated mice were analyzed to assess their immune response via the production of pro- and anti-inflammatory cytokines. Among the 26 cytokines evaluated by the multiplex analysis, we only observed significant differences in the secretion of RANTES, IL-10, Eotaxin, and IL-1 $\beta$  (Table 2). Indeed, we detected lower levels of RANTES in the three conditions when compared to control mice, corroborating the findings reported from another group.<sup>[55]</sup> Interestingly, there were higher levels of the anti-inflammatory cytokine IL-10 in the mice treated with the hybrid endometrial-derived hydrogel, whereas IL-10 secretion in Endo-NoDC and PM conditions was similar to untreated mice. Eotaxin secretion was higher in mice treated with Endo-NoDC and hybrid endometrial-derived hydrogels than in untreated mice. In addition, IL-1 $\beta$  levels were lower in the plasma of Endo-NoDC and PM groups. These findings support the notion that the production and release of some cytokines into the mice's bloodstream is driven by the specific composition of each hydrogel and its interactions with the adjacent tissue at the injection site.

Finally, we evaluated the persistence of the hydrogel and the extent of CD68<sup>+</sup> macrophage invasion 14 days post-injection. Congruent with our previous studies,<sup>[3]</sup> no Endo-NoDC hydrogels were found in the subcutaneous tissue of C57BL/6 mice after 14 days. Conversely, PM and hybrid endometrial-derived hydrogels persisted in the connective tissue underlying the dermis. With Masson's Trichrome staining, the fibers corresponding to the PM hydrogel acquired a pink color due to H&E counterstaining whereas the collagen I fibers of the EndoECM hydrogel component were stained aniline blue. As expected, the hybrid endometrial-derived hydrogel presented both pink and blue stains due to the presence of both components (Figure 5A). Immunohistochemical analysis for CD68 revealed an extensive macrophage infiltration in both PM and the hybrid endometrial-derived hydrogels at day 14 (Figure 5B). These observations substantiate that both PM and the hybrid endometrial-derived hydrogel, which exhibit superior rheological properties, require additional time for tissue repair and remodeling by macrophages.<sup>[56]</sup>

### 3. Discussion

The use of hydrogels has dramatically increased due to their numerous biological applications, including a 3D support for cell culture or vehicle for in vivo therapies. While synthetic hydrogels are fully customizable, they lack essential biomolecules to promote cell growth, migration, proliferation, function, differentiation, angiogenesis, antimicrobial or niche responses, mechanical support, and chemotaxis. In contrast, ECM hydrogels have emerged as promising alternatives since they contain proteins and secreted factors from the native tissue but do not contain antigen that elicit immune rejection.<sup>[34]</sup> Further, ECM hydrogels contribute to the establishment of more physiologically relevant organoid models that accurately model the in vivo responses in the native organ or tissue<sup>[57]</sup> and could be employed as treatment vehicles in vivo. Considering the advantages of both types of hydrogels, we combined synthetic and natural hydrogels to synthesize a hybrid hydrogel that mimics the 3D microenvironment

**Table 2.** Cytokines differentially expressed in the plasma of C57BL/6 mice 14 days after treatment with Endo-NoDC, PM, and hybrid endometrial-derived hydrogels. The differential expression was calculated with respect to the values in untreated mice. Up and down arrows represent respectively higher and lower significant expression in the treated group versus untreated mice. The equal symbol (=) indicates non-significant differences between groups. The immunological function of each cytokine is also described. N = 12 mice (4 per condition). *RANTES*: Regulated on Activation, Normal T Expressed and Secreted; *IL-10*: interleukin 10; *IL-1 $\beta$* : interleukin 1 $\beta$ .

Cytokine	Plasma levels (day 14) Endo-NoDC	Plasma levels (day 14) PM	Plasma levels (day 14) Hybrid endometrial-derived hydrogel	Biological functions
RANTES	↓	↓	↓	<ul style="list-style-type: none"> <li>✓ Produces pro-inflammatory cytokines and amplifies the inflammatory response.<sup>[75]</sup></li> <li>✓ Recruits and activates inflammatory cells (particularly, monocytes, lymphocytes, mast cells, and eosinophils).<sup>[76]</sup></li> <li>✓ Mediates various chronic conditions.<sup>[55,77]</sup></li> </ul>
IL-10	==	==	↑	<ul style="list-style-type: none"> <li>✓ Regulates the ECM. Protects against the excessive deposition of collagen during wound healing.<sup>[78]</sup></li> <li>✓ Enhances fibroblast function through increased hyaluronan production.<sup>[79]</sup></li> <li>✓ Re-establishes tissue integrity after injury in multiple tissues, including skin.<sup>[71]</sup></li> </ul>
Eotaxin	↑	==	↑	<ul style="list-style-type: none"> <li>✓ Mediates regenerative effects on the epithelium through interactions with fibroblasts and keratinocytes.<sup>[71]</sup></li> <li>✓ Maintains organ homeostasis (particularly in the liver).<sup>[72]</sup></li> </ul>
IL-1 $\beta$	↓	↓	==	<ul style="list-style-type: none"> <li>✓ Facilitates eosinophil chemotaxis, adhesion, and aggregation to promote tissue regeneration.<sup>[80]</sup></li> <li>✓ Mediates inflammation and innate immune responses.<sup>[73]</sup></li> <li>✓ Recruits immune cells during the early stages of wound healing.<sup>[73]</sup></li> <li>✓ Encourages proliferation and migration of fibroblasts that produce collagen and other ECM components for tissue repair.<sup>[73]</sup></li> <li>✓ Stimulates production of growth factors.<sup>[73]</sup></li> </ul>

of the native endometrial milieu.<sup>[20]</sup> In reproductive medicine, these types of hybrid hydrogels are promising for the development of therapeutic interventions for endometrial disorders.<sup>[58]</sup> The unique properties of hybrid hydrogels, including enhanced rheological characteristics and essential biochemical cues, will allow researchers and clinicians to bridge the knowledge and healthcare gaps associated with endometrial conditions, advancing the understanding of female reproductive physiology and/or restoring fertility.

In this study, we developed a hybrid endometrial-derived hydrogel by combining two different components at a 50:50 ratio: i) PuraMatrix (PM), a synthetic biomaterial that provides adjustable stiffness and viscosity; and ii) porcine EndoECM hydrogel, a natural matrix obtained through the decellularization of porcine endometrial tissue, that confers important biochemical cues for cell culture.<sup>[35]</sup> We performed a mechanical characterization of different hydrogel combinations by analyzing rheological properties (i.e., storage and loss modulus, complex viscosity, and oscillation stress) to gain insights into their viscoelastic properties<sup>[59]</sup> and determine their ability to provide 3D support in *in vitro* cell cultures. While the rheological properties of the Matrigel, EndoECM, and Matrigel + EndoECM (50:50) hydrogels were significantly lower than those of porcine endometrial tissue, the rheological properties of PM closely reflected those of the porcine endometrial tissue, indicating that the strength of the PM hydrogel network was equivalent to that of the porcine native endometrium. Combining PM and EndoECM hydrogel in a 50:50 ratio significantly increased the hydrogel stiffness, enhancing the rheological properties of the EndoECM hydrogel component to a degree where it faithfully replicates the mechanical characteristics of the porcine endometrial tissue. A physicomimetic microenvironment, like

the one we achieved with our hybrid endometrial-derived hydrogel, is essential for organoid culture and *in vivo* models, since it facilitates cell organization and differentiation.<sup>[60]</sup> Understanding the optimal balance of mechanical and biochemical cues required to support 3D cell cultures is crucial for advancing the development of more accurate and functional hEO models that mimic the responses the native endometrium.

As there is evidence suggesting an effect of the fibrotic component on essential characteristics of hydrogels,<sup>[61]</sup> we compared the fibers in the hybrid endometrial-derived hydrogel under SEM to those in PM and EndoECM hydrogels. As expected, the collagen fibers identified in EndoECM hydrogel and the RADA<sub>16</sub> peptides detected in PM sample were both present in the hybrid endometrial-derived hydrogel. There being no significant differences in fiber diameter between the hydrogels demonstrated the addition of PM did not compromise the EndoECM hydrogel morphology. Furthermore, the PM component of the hybrid endometrial-derived hydrogel created a 3D structure that filled the “gaps” between the collagen fibers of EndoECM hydrogel, increasing the surface area, and therefore, the physical support and capacity for cell adhesion.<sup>[41,61]</sup>

The matrisome refers to the complete set of ECM proteins in a particular sample, which are generally categorized as core matrisome (e.g., glycoproteins, collagens, and proteoglycans) and matrisome-associated proteins (e.g., ECM-affiliated proteins, regulators, and secreted factors).<sup>[29]</sup> These proteins have domains bind adhesion receptors that mediate cell-matrix adhesion and transduce signals to cells in a spatially organized and regulated fashion. Therefore, the preservation of ECM proteins in natural hydrogels can promote cell adhesion, proliferation, and differentiation rather than other biomaterials.<sup>[62]</sup> Herein, we show

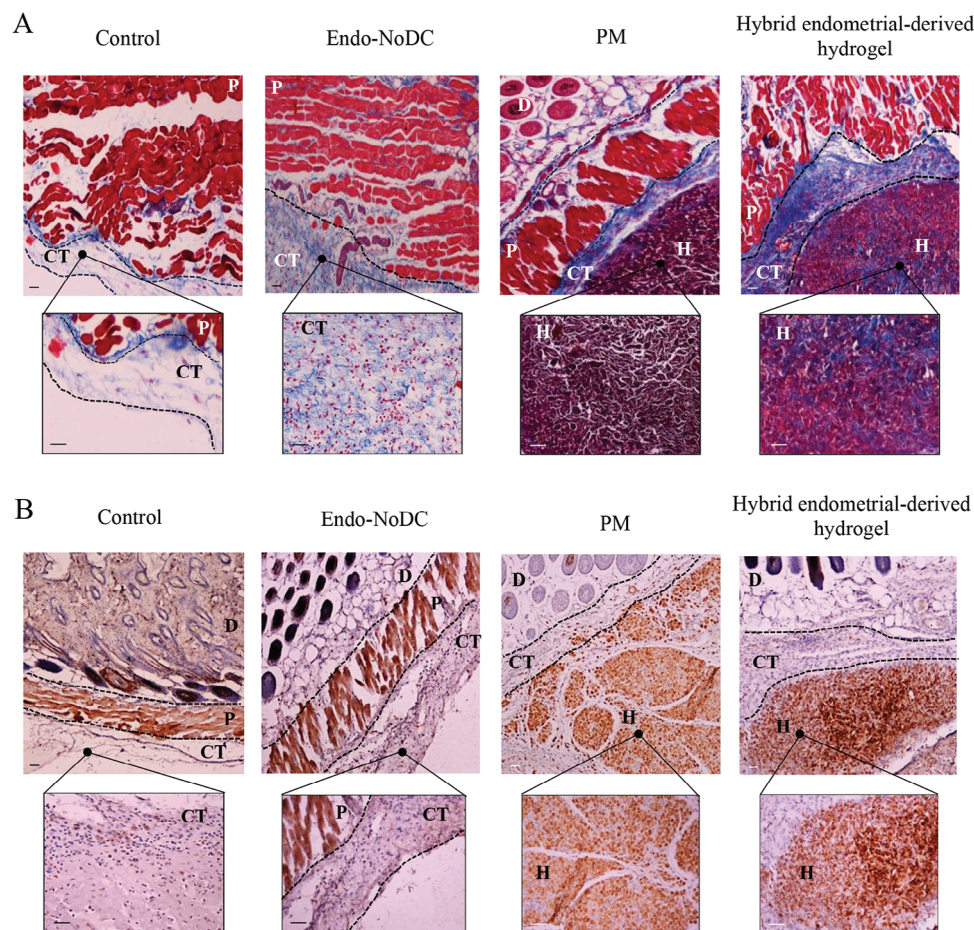


**Figure 5.** Evaluation of hydrogel persistence and CD68+ macrophage invasion in C57BL/6 mice 14 days after subcutaneous injections with the Endo-NoDC, PM, and hybrid endometrial-derived hydrogels. A) Masson's Trichrome staining of control, Endo-NoDC, PM, and hybrid endometrial-derived hydrogels. Aniline blue stains the collagen I fibers. B) Immunohistochemistry for CD68, which reveals a higher infiltration in PM and hybrid endometrial-derived conditions with respect to control and Endo-NoDC mice. Scale bar = 50  $\mu$ m. D: dermis; P: panniculus carnosus; CT: connective tissue; H: hydrogel.

there were no statistically significant differences in the proportion of core matrisome proteins nor matrisome-associated proteins between the EndoECM hydrogel and the EndoECM fraction of the hybrid endometrial-derived hydrogel. Both groups shared 33 proteins, including the most important structural components of the endometrial ECM (collagen type I-III, V, VI, XIV, XXVIII), several glycoproteins (including dermatopontin, Von Willebrand factor, laminin, and elastin), and ECM-associated proteins (including annexin, elastase, and protein S100) with key roles in wound healing, chemotaxis, immune response, and antibacterial functions.<sup>[35]</sup> Only six proteins of the EndoECM hydrogel were not preserved in the hybrid endometrial-derived hydrogel, including fibrinogen gamma chain (FGG), collagen type 4 alpha 1 and 2 (COL4A1, COL4A2), collagen type 5 alpha 3 (COL5A3), serpin peptidase inhibitor clade B member 1 (SERPINB1), and S100 calcium binding protein A9 (S100A9). Given that the EndoECM hydrogel component was diluted by a factor of 0.5 in the hybrid endometrial-derived hydrogel, the identification of these proteins may have been hindered by the limited sensitivity of the LC-MS/MS technique. Nevertheless, we confirm there was no significant loss in the biochemical com-

position of the hybrid endometrial-derived hydrogel compared to the porcine EndoECM hydrogel. The matrisome of our hybrid endometrial-derived hydrogel had 17 proteins in common with a previously described bovine EndoECM hydrogel.<sup>[28]</sup> These included not only structural proteins (collagens) but also other key ECM proteins (laminin, fibrinogen, fibronectin, transglutaminase, and S100 calcium binding protein A8). Meanwhile, and to our surprise, our hybrid endometrial-derived hydrogel only shared two specific proteins with the human EndoECM hydrogel (fibrillin, laminin)<sup>[38]</sup> and two other with the human native endometrium (annexin, laminin).<sup>[38]</sup> Specifically, the gamma 2 chain of laminin (LAMC2) is an integral part of the anchoring filaments that connect epithelial cells to the underlying basement membrane,<sup>[63]</sup> whereas fibrillin-1 (FBN1) serves as a structural component of calcium-binding microfibrils.<sup>[64]</sup> Moreover, annexin A2 (ANXA2) is involved in the regulation of cellular growth and signal transduction pathways.<sup>[65]</sup> Thus, despite the low number of proteins shared between the EndoECM hydrogel and native endometrium, the preservation of these native proteins may facilitate the adhesion of endometrial epithelial cells to the hybrid endometrial-derived hydrogel, thereby promoting

the formation of hEOs. The differences in the preservation of these proteins in the hybrid endometrial-derived hydrogel compared to other hydrogels may be due to the decellularization process. Our protocol employs a soft decellularization with 0.1% sodium dodecyl sulphate (SDS) and perfusion, whereas others use higher concentrations of detergents and adopt the immersion technique<sup>[28,38]</sup> that might affect the integrity and biochemical composition of the ECM. In this regard, our protocol is superior because it preserves the proteins of the native tissue.

Concurrent to our proteomic results, we found that the hybrid endometrial-derived hydrogel, but not the PM hydrogel alone, was able to support the 7-day hEO culture. This is likely due to the biochemical cues provided by the EndoECM hydrogel component. In addition, the hEOs grown in the hybrid endometrial-derived hydrogel maintained the same histological characteristics as the control hEOs in terms of E-cadherin, Vimentin, and Ki67 marker expression. Conversely, the laminin expression was remarkably different in hEOs cultured in our hybrid endometrial-derived hydrogel, with a diffuse laminin signal inside the organoids, possibly associated to traces of the hybrid endometrial-derived hydrogel. This characteristic can be of interest to pursue novel tissue engineering applications, as natural ECM hydrogels offers more flexible and adaptable bioplat-forms for organoid culture. These organoids can be modified and engineered to suit specific tissue regeneration needs, driving the creation of custom-designed endometrial models for transplantation.<sup>[66]</sup>

Unlike other bioengineering studies that employed undifferentiated organoids,<sup>[31,33,41,42]</sup> we corroborated the suitability of the hybrid endometrial-derived hydrogel to promote hEOs differentiation to secretory and gestational phases. During the differentiation process, hEOs secrete a plethora of proteins into the culture media, including SPP1, which is particularly relevant due to its involvement in implantation and placentation.<sup>[48]</sup> As with our study, previous works have performed ELISA to characterize the differences between the SPP1 secretion from differentiated and undifferentiated hEOs.<sup>[6,67]</sup> The significant up-regulation of endometrial receptivity biomarkers (*SPP1*, *PAEP*, *LIF*, *17HSDβ2*)<sup>[52–56]</sup> together with the repression of the progenitor cell marker *SOX9*<sup>[6,55,56]</sup> confirmed a higher efficiency of the hEO differentiation in the hybrid endometrial-derived hydrogel. Altogether, the EndoECM hydrogel component of the hybrid endometrial-derived hydrogel provides a more suitable microenvironment for endometrial cells, with a matrisome that enhances the ability to differentiate to secretory and gestational phases, and superior rheological properties which can influence signaling pathways that regulate gene expression and cell differentiation.<sup>[60,68]</sup> Since the stiffness of the hybrid endometrial-derived hydrogel closely matches the native endometrial stiffness, it can provide better support the differentiation of endometrial cells into the appropriate cell types for that phase.

Once we assessed the *in vitro* functionality of our hybrid endometrial-derived hydrogel, we sought to evaluate its *in vivo* compatibility for future therapeutic applications. Therefore, we used an immunocompetent murine model (C57BL/6) to identify possible immune reactions after a single subcutaneous injection of Endo-NoDC (positive control), PM, or the hybrid endometrial derived hydrogel. While the biocompatibility of porcine EndoECM hydrogel was evidenced by the lack of significant adverse

immune reactions after 48 h,<sup>[3,4]</sup> the exclusively synthetic PM and hybrid endometrial-derived hydrogels offer superior mechanical properties, enabling them to persist *in vivo* for extended periods of time.<sup>[69]</sup> For this reason, we evaluated the immune response of injected mice after 2, 7, and 14 days.

The hematocrit provides information about red and white blood cell counts, and can be used to flag systemic changes in the immune system. Differences in hematocrit values can be considered an additional biomarker in the diagnosis of infectious diseases or transplant rejection.<sup>[70]</sup> Our data shows no significant changes in hematological parameters in any of the three conditions with respect to the values from C57BL/6 female mice,<sup>[54]</sup> except for some decreases in erythrocyte and platelet counts that are probably due to the coagulation process of the subcutaneous wound generated by the hydrogel injection. Consistent with these findings, we only identified significant differences in the secretion of 4 out of 26 cytokines in the plasma of injected mice: RANTES, IL-10, Eotaxin, and IL-1 $\beta$ . RANTES stimulates the production of other pro-inflammatory cytokines and the amplification of the inflammatory response. RANTES is overexpressed in renal graft rejection,<sup>[55]</sup> but in this study, RANTES levels were significantly lower in treated mice than untreated controls. IL-10 secretion was highest in the mice that received the hybrid endometrial-derived hydrogel, corroborating the suitable biological properties of this hydrogel. IL-10 is an anti-inflammatory cytokine involved in the regulation of the ECM, which plays a key role in epithelial regeneration by stimulating fibroblasts to produce hyaluronan, among other functions.<sup>[62–64]</sup> Thus, an increased secretion of IL-10 can promote a more favorable environment for tissue healing and regeneration, ultimately promoting tissue repair and recovery.<sup>[71]</sup> Eotaxin levels were higher in the mice treated with Endo-NoDC and the hybrid endometrial-derived hydrogel than in untreated mice, likely because they promote the recruitment of eosinophils to the subcutaneous tissue during the repair process.<sup>[72]</sup> In addition to Eotaxin, IL-1 $\beta$  is also involved in tissue repair by promoting fibroblast proliferation and migration, along with the production of growth factors.<sup>[73]</sup> Multiplex analyses showed a lower IL-1 $\beta$  secretion in Endo-NoDC and PM conditions, whereas IL-1 $\beta$  levels in the mice who received the hybrid endometrial-derived hydrogel were closer to those of untreated mice. Collectively, these results suggest that the hybrid endometrial-derived hydrogel does not produce significant systemic alterations in the murine immune system but induces the differential expression of tissue regeneration-related cytokines, such as IL-10 and IL-1 $\beta$ .

After 14 days, the histological studies showed the presence of remnant PM and hybrid endometrial-derived hydrogels surrounded by significant macrophage infiltration in the subcutaneous tissue. In contrast, no Endo-NoDC hydrogel was detected. Due to their higher rheological properties, the fully synthetic (PM) and hybrid endometrial-derived hydrogels require more time to be remodeled by the macrophage system and therefore can persist *in vivo* for longer period of time.<sup>[56]</sup> Increased *in vivo* stability may be beneficial for several bioengineering applications, such as prolonging support of cellular material or sustaining local release of therapeutic agents.<sup>[20]</sup> It is important to note that, although the presence of these hydrogels was maintained, it did not negatively alter the immune system of immunocompetent mice, as shown by our blood and plasma analyses.

The present study has several limitations. As a pilot study, our research is limited by relatively few hEOs. Therefore, increasing the number of endometrial biopsies might strengthen these findings. Despite demonstrating the hydrogel biocompatibility in immunocompetent mice, further studies should validate its role as a vehicle for cells or other biological products (e.g., growth factors).

In summary, the hybrid endometrial-derived hydrogel, created through a combination of PM and porcine EndoECM hydrogel (50:50), exhibits enhanced mechanical properties and robust preservation of the tissue-specific ECM biomolecules found in the native endometrium, relative to the other endometrial hydrogels described in the literature. In our *in vitro* studies, the hybrid endometrial-derived hydrogel has proved to be a suitable biomaterial for supporting the efficient differentiation of hEOs into secretory and gestational phases. Our *in vivo* results confirmed the xenogeneic biocompatibility and persistent stability of the hybrid endometrial-derived hydrogel at the injection site after 14 days, positioning it as a promising tool for translational bioengineering applications in reproductive medicine.

## 4. Experimental Section

**Experimental Design:** A detailed characterization of hydrogels was performed based on PM and EndoECM by rheology, SEM, and proteomic analyses. Based on its mechanical and biochemical properties, this work selected the PM + EndoECM hydrogel (50:50) to evaluate its suitability for culturing simple and differentiated hEOs (secretory and gestational). Next, to test its biocompatibility, C57BL/6 female mice received a single subcutaneous injection with 200  $\mu\text{L}$  of EndoECM-NoDC hydrogel, PM, or the hybrid endometrial-derived hydrogel. The mice's local and systemic immune responses were analyzed after 2, 7, and 14 days (Figure 6).

**Hydrogel Characterization of the Hybrid Endometrial-Derived Hydrogel—Porcine Uterus Decellularization, Endometrial Isolation, and EndoECM Hydrogel Setup:** Female porcine reproductive tracts were donated by a slaughterhouse in Mercavelencia, Spain. Uterine horns were decellularized following a two-cycle protocol, as previously described.<sup>[35,74]</sup> Briefly, 0.1% SDS and 1% Triton X-100 were perfused through the uterine artery using a peristaltic pump (Cole-Parmer Instruments, Fisher Scientific). Decellularized horns were stored at  $-80\text{ }^{\circ}\text{C}$  until further processing. The horns were cut transversally into 1 mm thick disks, and the endometrial tissue was manually microdissected under a stereomicroscope (SMZ800, Nikon) and then stored at  $-80\text{ }^{\circ}\text{C}$ .<sup>[37]</sup> To remove residual DNA and detergents the thawed endometrial tissue was washed in cold PBS (10 mL  $\text{g}^{-1}$  tissue) and incubated for 1 h in 5  $\mu\text{g mL}^{-1}$  DNase I solution (D5025, Sigma-Aldrich) at room temperature (RT). Next, endometrial tissue was flash-frozen in a mortar with liquid  $\text{N}_2$ , milled manually, and lyophilized (Lyocquest-85, Telstar, Valencia's Polytechnic University) over 96 h at 20 Pa. This lyophilized powder was digested with 0.01 M HCl (H1758, Sigma-Aldrich) and 0.1% pepsin (P7000, Sigma-Aldrich) then neutralized with 10% (v/v) 0.1 M NaOH (S8045, Sigma-Aldrich), 11.11% (v/v) 10X PBS (P5493, Sigma-Aldrich), and 1X PBS until the desired concentration (8.25 mg  $\text{mL}^{-1}$ ) was obtained. Aliquots of the resulting EndoECM hydrogel were stored at  $-80\text{ }^{\circ}\text{C}$ .

**Hydrogel Characterization of the Hybrid Endometrial-Derived Hydrogel—Hybrid Endometrial-Derived Hydrogel Preparation:** The 1% w/v (10 mg  $\text{mL}^{-1}$ ) PM (10255252, Fisher Scientific) underwent bath sonication for 30 min to decrease its viscosity. The 1% PM was combined with 8.25 mg  $\text{mL}^{-1}$  EndoECM hydrogel at 50:50 ratios to prepare the hybrid endometrial-derived hydrogel (final concentration of 5 mg  $\text{mL}^{-1}$  PM and 4.12 mg  $\text{mL}^{-1}$  EndoECM hydrogel). To ensure a homogeneous mixture of both solutions, the hybrid endometrial-derived hydrogel underwent an additional 10-min sonication and was stored at  $4\text{ }^{\circ}\text{C}$  until use.

**Hydrogel Characterization of the Hybrid Endometrial-Derived Hydrogel—Rheological Analyses:** The mechanical characterization of the biomateri-

als was performed using a 25 mm parallel-plate geometry on a rotational rheometer (Discovery Hybrid Rheometer DHR, TA Instruments, DE, USA). For rheological testing, 300  $\mu\text{L}$  of Matrigel, EndoECM hydrogel, Matrigel + EndoECM hydrogel (50:50), PM + EndoECM hydrogel (25:75), PM + EndoECM hydrogel (50:50) and PM samples were placed between plates, after prewarming the lower disk to  $37\text{ }^{\circ}\text{C}$ . Samples with PM were previously sonicated at  $37\text{ }^{\circ}\text{C}$  for 10 min to homogenize the hydrogels. For the porcine endometrial control tissue, a 25 mm of tissue was employed. To obtain the temporal evolution of the storage and loss modulus, an oscillation time procedure was performed, where samples were subjected to a strain of 1% and a frequency of 1 Hz for 60 s. To obtain the storage modulus and complex viscosity, an oscillation frequency procedure was performed, where samples were subjected to a strain of 1% followed by a logarithmic frequency sweep ranging from 0.1 to 10 Hz. Only the results for a frequency of 1 Hz were presented. To obtain the oscillation stress, a flow sweep procedure was performed, where samples were subjected to a logarithmic shear rate sweep ranging from 1 to 100  $\text{s}^{-1}$ . Only results for a shear rate of 10  $\text{s}^{-1}$  were presented. All samples were measured at physiological temperature ( $37\text{ }^{\circ}\text{C}$ ). Data were obtained from three biological repeats ( $n = 3$ ) for each experimental setup.

**Hydrogel Characterization of the Hybrid Endometrial-Derived Hydrogel—Scanning Electron Microscopy:** The ultrastructure of EndoECM, PM, and PM + EndoECM (50:50) hydrogels was evaluated using SEM. Samples were processed in the proteomics facility of SCSIE at the University of Valencia. Hydrogels were fixed in 2.5% glutaraldehyde in PBS (Sigma-Aldrich, 25%) for 24 h, washed and kept in PBS at  $4\text{ }^{\circ}\text{C}$ . All hydrogels were then treated with 2% osmium tetroxide for 2 h and dehydrated in a graded series of alcohol (30, 50, 70, 90, 100% ethanol) for 30 min per wash; and kept in 100% ethanol overnight at  $4\text{ }^{\circ}\text{C}$ . Hydrogels were washed thrice in 100% ethanol for 30 min and critical point dried using a AutosamdriR 814 Critical Point Dryer (Tousimis). Carbon dioxide ( $\text{CO}_2$ ), at high pressure (1200 pound-force per square inch, psi), was used as the transitional medium at a maximum heating temperature of  $40\text{ }^{\circ}\text{C}$ . Dried samples were coated with gold-palladium for 2 min using a SC7640 Sputter Coater (Quorum technologies) and images were captured with a SEM FEG Hitachi S-4800 (SCSIE University of Valencia, Spain). To analyses fiber diameter, 10 measurements were taken per sample (50.0 k images) using FIJI-ImageJ software.

**Hydrogel Characterization of the Hybrid Endometrial-Derived Hydrogel—Proteomics Analysis:** The proteomic analysis was performed in the SCSIE proteomics facility of the University of Valencia, using a volume of 50  $\mu\text{L}$  of EndoECM hydrogel and 50  $\mu\text{L}$  of hybrid endometrial-derived hydrogel. To identify the amino-acid sequence of PM in the hybrid endometrial-derived hydrogel, the sample was precipitated with acetonitrile (ACN) to separate the PM peptides (analyzed directly from the supernatant without digesting) from the proteins of the EndoECM hydrogel. Briefly, the ACN was added to the samples in a 1:1 ratio and left overnight at  $4\text{ }^{\circ}\text{C}$ . Then, the samples were centrifuged (5 min, 5000 rpm) and the supernatants were dried in a speed vacuum. Pellets were resuspended in 50  $\mu\text{L}$  of 2% ACN with 0.1% trifluoroacetic acid (TFA) and sonicated for 5 min. After quantification in a NanoDrop spectrophotometer (Thermo Fisher Scientific) at 280 nm absorbance, the samples were diluted with 0.1% TFA and 2% ACN to a final volume of 2  $\mu\text{L}$ . For protein identification, 50  $\mu\text{L}$  of the EndoECM and the hybrid endometrial-derived hydrogels samples were denatured and loaded onto a 12% SDS-PAGE gel (Bio-Rad) for electrophoresis (200 V, 10 min). Gels were fixed, stained with colloidal Coomassie (Bio-Rad), and cut into three fragments so every gel band could be digested separately with 2000 ng sequencing-grade trypsin (Promega) at  $37\text{ }^{\circ}\text{C}$ . The digestion was neutralized with TFA 1% and all peptide solutions were subjected to a final double extraction with ACN before being dried in a rotatory evaporator and resuspended with 2% ACN and 0.1% TFA to an estimated final concentration of 0.3  $\mu\text{g mL}^{-1}$ .

Isolated peptides were identified and quantified using a LC-MS/MS workflow for data-dependant acquisition. 2  $\mu\text{L}$  of the peptide mixture samples were loaded onto a trap column (ChromXP C18, 3  $\mu\text{m}$  120  $\text{\AA}$ , 350  $\mu\text{m}$ , 0.5 mm; Eksigent) and desalted with 0.1% TFA at 5  $\mu\text{L min}^{-1}$  for 5 min. Peptides were then loaded onto an analytical column (3  $\mu\text{m}$  C18-CL 120  $\text{\AA}$ , 0.075  $\times$  150 mm; Eksigent) equilibrated in 5% ACN and 0.1% formic acid

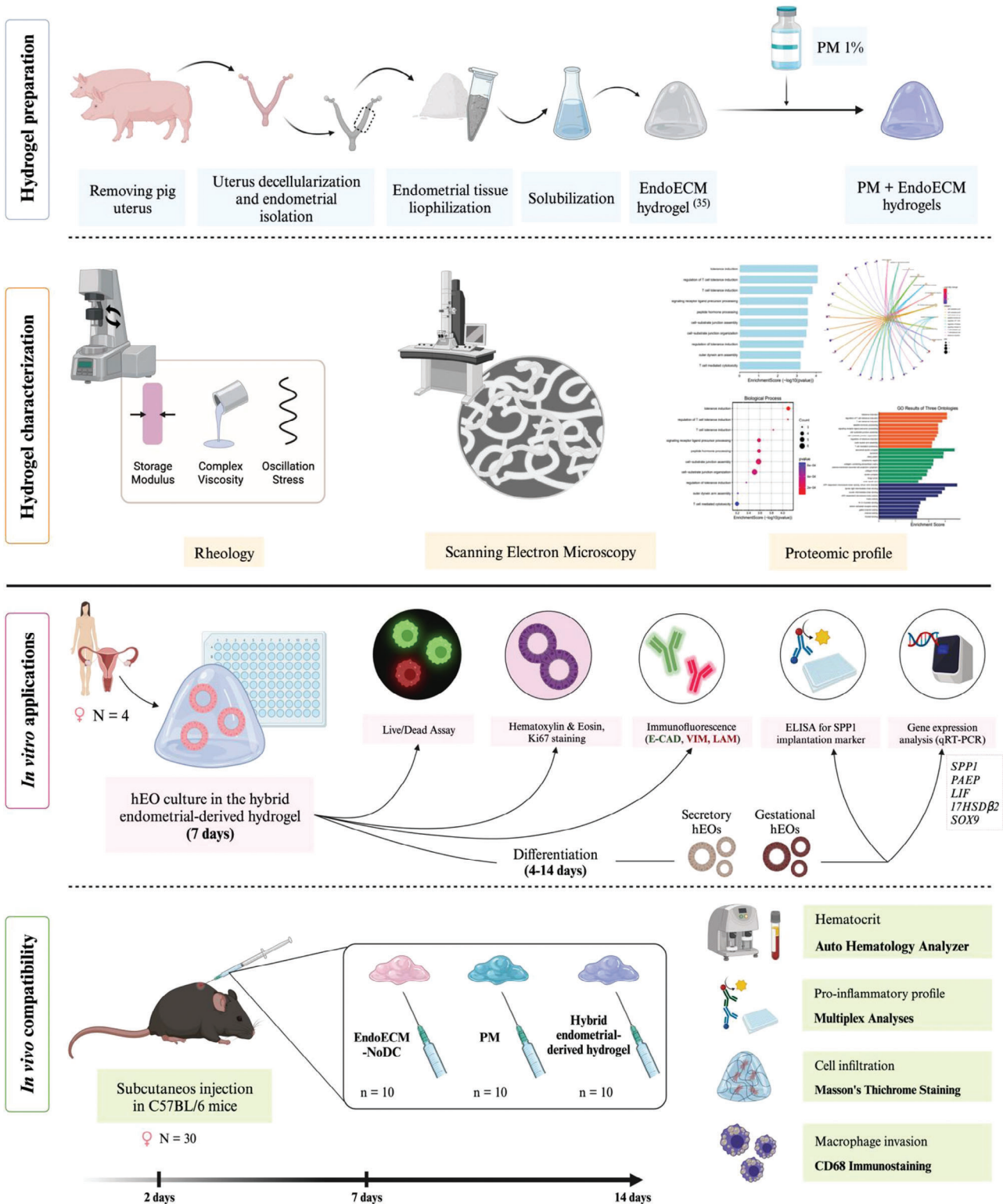


**Figure 6.** Experimental design. Characterization of the hybrid endometrial-derived hydrogel and its applications in vitro and in vivo. Created with BioRender.com. PM: PuraMatrix; EndoECM: decellularized endometrial extracellular matrix hydrogel; hEOs: human endometrial organoids; E-CAD: E-cadherin; VIM: vimentin; LAM: laminin; qRT-PCR: real-time quantitative reverse transcription PCR; EndoECM-NoDC: non-decellularized endometrial extracellular matrix hydrogel.

(FA). Elution was carried out with a linear gradient of 5 to 75% B in A for 20 min. (A: 0.1% FA; B: ACN, 0.1% FA) at a flow rate of 300 nL min<sup>-1</sup>. Peptides were analyzed in a mass spectrometer nanoESI qTOF (6600plus TripleTOF, ABSCIEX) with source type ionization mode.

The Paragon algorithm of ProteinPilotv 5.0 was used to search the Swiss Prot database (210126), Uniprot mamalia (210806) with the inclusion of the sequence of the peptide PM (ACN-(RADA)<sub>4</sub>-CNH<sub>2</sub>). The database parameters varied depending on the specific process. For PM peptide identification, the following parameters were used: no digestion, no cyst-alkylation, taxonomy not restricted, acetylation emphasis, search effort set to “through” and “FDR calculation.” For EndoECM hydrogel peptide identification, the parameters were: trypsin specificity, cyst-alkylation, taxonomy not restricted, the search effort set to through and FDR calculation.

The Pro group algorithm (AB Sciex) was employed to determine which groups of proteins derived evidence from largely the same spectra of reported peptides and which are considered redundant. Peptides and proteins exceeding unused scores of >0.88 were identified with a confidence level of ≥80%. Mass spectrometry data from the hydrogels were combined and searched against the UniprotMammals database (SCSIE at the University of Valencia).

Peptides were grouped according to their parent protein and the individual coverage (% cov) was calculated as an indicator of relative protein abundance. The complete list of peptides identified in the EndoECM (Table S1, Supporting Information) and hybrid endometrial-derived hydrogels (Table S2, Supporting Information) can be found in the Supplementary Material. Functional analysis of the detected proteins was conducted with the PANTHER classification system, using the Gene Ontology database (GO: biological processes, cellular component, and molecular function). The ECM-related biological processes and molecular functions assigned to each protein are presented in Table S3, Supporting Information.

**Hydrogel Characterization of the Hybrid Endometrial-Derived Hydrogel—Comparison of Proteomics Analyses:** The matrisome of the hybrid endometrial-derived hydrogel was compared to the previously characterized matrisomes of the bovine EndoECM hydrogel,<sup>[28]</sup> human EndoECM hydrogel,<sup>[38]</sup> and native endometrium tissue.<sup>[38]</sup> The relationships between the proteins in each matrisome were examined through Interactienn webpage. Finally, a functional GO analysis of the detected proteins was conducted with the g:Profiler tool.

**Biological Applications of the Hybrid Endometrial-Derived Hydrogel—Organoid Development from Endometrial Biopsies:** This study was approved by the Ethical Committee of the IVI Foundation (2107-FIVI-073-IC, Valencia, Spain). All participants provided written informed consent. Endometrial biopsies ( $n = 4$ ) were collected by laparoscopy from healthy oocyte donors at the IVI Valencia (Valencia Spain), following controlled ovarian stimulation and on the day of the oocyte retrieval. Biopsies were washed in DMEM/F-12 without phenol red (GibcoTM, 11039021) and fragmented into 0.5–1 mm<sup>3</sup> pieces that were enzymatically digested in a collagenase-dispase solution [15 mL RPMI 1640 medium (GibcoTM, 21875034), 50 U mL<sup>-1</sup> Dispase II (Sigma-Aldrich, D4693) 0.4 mg mL<sup>-1</sup> collagenase V (Sigma-Aldrich, C9263), and 10% newborn calf serum (Biowest, S0750)]. After an overnight incubation at 4 °C, the digestion was stopped by adding 30 mL RPMI 1640 medium. To isolate the glandular elements, the supernatant was passed through 100 μm cell sieves (CorningTM, 431752), which were then inverted and backwashed with 12 mL advanced DMEM/F12 medium (GibcoTM, 12634010). After centrifugation, the pellet was resuspended in 15% advanced DMEM/F12 and 85% ice-cold Matrigel (Corning, 354234). Drops of 20 μL were plated into 48-well plates (Corning TM, 3548), set at 37 °C for 30 min, and cultured in organoid expansion medium (ExM). ExM contains advanced DMEM/F12; N2 supplement 1X (GibcoTM, 17502048); B27 supplement minus vitamin A 1X (GibcoTM, 12587010); Primocin, 100 μg mL<sup>-1</sup> (InvivoGen, ant-pm-1); 1.25 mM N-acetyl-L-cysteine (Sigma-Aldrich, A9165); 2 mM L-glutamine (Sigma-Aldrich, G7513); 50 ng mL<sup>-1</sup> recombinant human EGF (PeproTech, AF-100-15); 100 ng mL<sup>-1</sup> recombinant human Noggin (PeproTech, 120-10c); 500 ng mL<sup>-1</sup> recombinant human R-Spondin-1 (PeproTech, 120-38); 100 ng mL<sup>-1</sup> recombinant human FGF-10 (PeproTech, 100-26); 50 ng mL<sup>-1</sup> recombinant human HGF (PeproTech, 100-39); 500 nM ALK-4, -5, -7 inhibitors (A83-01, PeproTech, 9094360); and

10 nM nicotinamide (Sigma-Aldrich, N0636).<sup>[6]</sup> Medium was changed every 2 to 3 days. Organoids from all biopsies were cultured in vitro for 3–5 passages and frozen to generate enough stock for the subsequent experiments.

**Biological Applications of the Hybrid Endometrial-Derived Hydrogel—In Vitro Culture of Human Endometrial Organoids:** Human endometrial organoids from passages 3–5 ( $n = 4$ ) were used for 3D culture. After 7-day culture in Matrigel, endometrial organoids were passaged according to Turco's methodology<sup>[6]</sup> with slight modifications. For intermediate steps, this work used distilled water (dH<sub>2</sub>O) with 20% sucrose (Sigma-Aldrich, S9378). After centrifugation, the pellet containing the hEOs was resuspended in dH<sub>2</sub>O + 20% sucrose and the hybrid endometrial-derived hydrogel. Drops of 50 μL were plated into 96-well round bottom plates (Labclinics, PLC34296), set at 37 °C for 30 min, and cultured in 150 μL of ExM. Next, 100 μL well<sup>-1</sup> of ExM was refreshed to neutralize the acidic pH of the hybrid endometrial-derived hydrogel. Alternatively, for the control condition, 50 μL drops containing 15% advanced DMEM/F12 and 85% Matrigel were plated, set at 37 °C for 30 min, and cultured in 150 μL of ExM. In both conditions, the ExM was changed every 2 to 3 days. The total duration of the culture period was 7 days.

**Biological Applications of the Hybrid Endometrial-Derived Hydrogel—Differentiation of Human Endometrial Organoids:** Organoids in passage 5–7 were thawed and cultured with ExM for 7 days to retain their undifferentiated status (control organoids). For differentiation assays, the ExM was supplemented with 10 nM estradiol (Sigma-Aldrich, E4389) for the first 48 h followed by 10 nM estradiol, 1 μM progesterone (Sigma-Aldrich, P7556), and 1 μM cyclic adenosine monophosphate (cAMP; Sigma-Aldrich, B7880) for 4 days to promote differentiation to the secretory phase. To obtain gestational organoids, 20 ng mL<sup>-1</sup> recombinant human prolactin (PeproTech, Cranbury, NJ, USA, 100-07) and 20 ng mL<sup>-1</sup> recombinant human placental lactogen (R&D, Minneapolis, MN, USA, 5757-PL) were added to secretory ExM for an additional 8 days.

**Biological Applications of the Hybrid Endometrial-Derived Hydrogel—LIVE/DEAD Assay:** The LIVE/DEAD Cell Imaging Kit (Thermo Fisher Scientific, R37601) was used to confirm hEO cell viability on day 7, according to the manufacturer's protocol. This work used 100 μL of the 2X working solution for every two wells. After 15 min, PBS 1X was added to stop the reaction and samples were immediately examined under an inverted Zeiss Axio Vert.A1 microscope (Zeiss, Oberkochen, Germany) at ×5 and ×10 magnifications to assess cell viability.

**Biological Applications of the Hybrid Endometrial-Derived Hydrogel—Histology, Immunohistochemistry, and Immunofluorescence of Human Endometrial Organoids:** To dissolve the hybrid endometrial-derived hydrogel and release the organoids, the drops were incubated with 150 μL well<sup>-1</sup> cell recovery solution (Thermo Fisher Scientific, 11560446) for 60 min at 4 °C. The organoids were transferred to an Eppendorf tube for centrifugation (600 × g for 6 min), and the pellet was fixed with 4% formaldehyde (Sigma-Aldrich, 1.00496) during 30 min at 4 °C. Three cycles of centrifugation and resuspension in 1 mL PBS 1X (Sigma-Aldrich, P3813) were performed before mixing the organoids with 200 μL HistoGel (Thermo Fisher Scientific, HG-4000-012) preheated to 55 °C. Samples were dehydrated in a series of alcohols, embedded in paraffin, and cut into 4 μm sections. H&E staining were performed according to the manufacturer's protocol to visualize glandular structures.

Cell proliferation was evaluated as previously described.<sup>[39]</sup> Briefly, samples were incubated with anti-Ki67 primary antibody (Dako, M7240, 1:100) overnight at 4 °C. After blocking endogenous peroxidase activity, slides were incubated with labeled-polymer horseradish peroxidase substrate-chromogen and counterstained with haematoxylin. Proliferative index was obtained by counting positive and total cell nuclei in 5 photos per condition (hybrid endometrial-derived hydrogel, Matrigel) by three independent observers and compared.

The expression and localization of E-cadherin, vimentin, and laminin were assessed by immunofluorescence staining. Organoids sections were deparaffinized, rehydrated, and subjected to heat-induced epitope retrieval with 10 mM sodium citrate buffer (pH 6) for 20 min in a 95 °C water bath. Samples were permeabilized with TBS-Tween 0.05% and blocked with TBS-Tween 0.05% containing 3% bovine serum albumin (product ref



**Table 3.** Primer sequences for qRT-PCR. *SPP1*: Secreted Phosphoprotein 1; *PAEP*: Progesterone Associated Endometrial Protein; *LIF*: Leukemia Inhibitory Factor; *17HSDβ2*: Hydroxysteroid 17-Beta Dehydrogenase; *SOX9*: SRY-related HMG-box; *GAPDH*: Glyceraldehyde-3-Phosphate Dehydrogenase.

GENE	Forward Sequence	Reverse Sequence
<i>SPP1</i>	CGAGGTGATAGTGTGGTTATG	GTCTGTAGCATCAGGGTACT
<i>PAEP</i>	ATGGCGACCAACAACATC	CTCTCCAAGGACCTTCTTCT
<i>LIF</i>	AACTGGCACAGCTCAATG	ATAGCTTGCCAGGTTGTTG
<i>17βHSD2</i>	TGAATGTCAGCAGCATGG	GGAAAGCTCCAGTCTCATAAC
<i>SOX9</i>	GACTCGCCACTCTCTCT	GTCGGTTTTGGGGTGGT
<i>GAPDH</i> (housekeeping)	AACGTGTCAGTGGTGACCTGA	ACCACCTGTTGCTGTAGCCAA

for 1 h at RT. To detect E-cadherin and vimentin colocalization, organoids were incubated with anti-E-CAD (Werfen, #3195, 1:300) overnight at 4 °C, followed by the Alexa Fluor 488-conjugated goat anti-rabbit IgG secondary antibody (Invitrogen, A11034, 1:500) for 45 min at RT, anti-VIM (Abcam, ab92547, 1:300) for 30 min at RT, and the corresponding Alexa Fluor 568-conjugated goat anti-rabbit IgG1 cross-absorbed secondary antibody (Invitrogen, A21124, 1:500) for 45 min at RT. Alternatively, to evaluate the expression of laminin, organoids were incubated with anti-LAM (Abcam, ab11575, 1:200) overnight at 4 °C, followed by Alexa Fluor 488-conjugated goat anti-mouse IgG1 secondary antibody (Invitrogen, A21121, 1:500) for 45 min at RT. In both analyses, the samples were counterstained with DAPI (Thermo Fisher Scientific, 62 248). Images were captured using a Nikon Eclipse 80i microscope (Nikon, Leuven, Belgium) and processed with FIJI-ImageJ software (Rasband, USA).

**Biological Applications of the Hybrid Endometrial-Derived Hydrogel—Enzyme-Linked Immunosorbent Assay:** Organoid secretion of the implantation marker *SPP1* was assessed by ELISA. Culture media from the undifferentiated, secretory, and gestational hEOs in Matrigel and the hybrid endometrial-derived hydrogel were collected. *SPP1* Human ELISA (Invitrogen, Eugene, OR, USA, BMS2066) was performed according to the manufacturer's instructions.

**Biological Applications of the Hybrid Endometrial-Derived Hydrogel—qRT-PCR Analyses:** Organoid gene expression of implantation and placental biomarkers including *SPP1*, *PAEP*, *LIF*, *17βHSD2*, and *SOX9* was evaluated by qRT-PCR using a StepOnePlus system (Applied Biosystems, Waltham, MA, USA, 4 376 600). Total RNA was extracted from control and differentiated hEOs grown in Matrigel or the hybrid endometrial-derived hydrogel ( $n = 4$ /group) using the Quick-RNA Micro Prep kit (Zymo Research, R1050). Specific primers used for qRT-PCR are listed in **Table 3**. Relative gene expression levels were normalized to *GAPDH* housekeeping gene expression using the  $\Delta\Delta C_t$  method and presented as a fold change with respect to the undifferentiated organoids.

**Biological Applications of the Hybrid Endometrial-Derived Hydrogel—In Vivo Biocompatibility Assays:** All experiments were performed in accordance with the European Union's Directive 2010/63/EU and the Ethics Committee for Animal Welfare of University of Valencia (A-20230113112219). Following the group's previous study,<sup>[3]</sup> 200  $\mu\text{L}$  of either 8.25  $\text{mg mL}^{-1}$  EndoECM-NoDC hydrogel, 1% PM, or the hybrid endometrial-derived hydrogel were injected in the dorsal subcutaneous space of immunocompetent female C57BL/6 mice ( $N = 10$ /group). This work evaluated scaffold morphology, local and systemic immune responses in mice at day 2 ( $N = 3$  mice/condition), 7 ( $N = 3$  mice/condition), and 14 days post-injection ( $N = 4$  mice/condition). Specifically, Masson's Trichrome staining and immunolabeling of the CD68 pan-macrophage marker (CD68 polyclonal antibody, ab125212, ABCAM, 1:200 dilution) were performed according to previous studies.<sup>[35]</sup> Additionally, the hematocrit and pro-inflammatory profile of mice were evaluated through blood and plasma, respectively. For each animal, 20  $\mu\text{L}$  of blood was combined with 2  $\mu\text{L}$  EDTA and analyzed with an Auto Hematology Analyzer – Element HT5-HESKA. In parallel, 25  $\mu\text{L}$  plasma was employed for multiplex analysis using the Cytokine & Chemokine 26plex-Mouse ProcartaPlex (EPX260-26088-901, Thermo Fisher Scientific) with Luminex xMAP Technology.

**Statistical Analysis:** All statistical analysis were performed with GraphPad Prism v6 (GraphPad software Inc., USA) software after verifying the normality of data distribution. Rheological results were analyzed by Oneway ANOVA. Fiber diameters measured by SEM were analyzed using the Student's *t*-test. Both ELISA and RT-qPCR results were normalized to their corresponding condition and analyzed using the Student's *t*-test. Multiplex and hematocrit results were analyzed by ordinary two-way ANOVA. Statistically significant differences are indicated by \*, \*\*, \*\*\*, or \*\*\*\*, indicating a *p*-value below 0.05, 0.01, 0.001, or 0.0001, respectively.

## Supporting Information

Supporting Information is available from the Wiley Online Library or from the author.

## Acknowledgements

The authors thank Mercavalencia for donating the sow uteri necessary to produce the EndoECM hydrogel, the staff of the animal facilities of the Central Research Unit of the Faculty of Medicine of the University of Valencia, and the scientific team from Hospital Peset for the multiplex analyses. Finally, the authors thank Rosalba Lopez for her editing services in preparing this manuscript for publication. Funding: This work was supported by Instituto de Salud Carlos III and co-founded by the European Union (Fondo Social Europeo), «El FSE invierte en tu futuro» (PI21/00305 [IC]) through the Miguel Servet Program (CP20/00120 [HF]; CP19/00149 [IC]), Ministerio de Universidades (FPU20/00251 [MGÁ], FPU19/04850 [ARE], FPU18/06327 [EFH], MS21-142 [CBF]), Generalitat Valenciana (CIAPOT/2022/29 [MAH], CIPROM/2021/058 [AP and IC]), and Vicerrectorado de Investigación de la Universitat Politècnica de València (PAID-10-22 [FGR]).

## Conflict of Interest

The authors declare no conflict of interest.

## Author contributions

H.F. and I.C. contributed equally to this work. F.G.R. and C.M.R. conducted the rheological experiments. M.G.Á. performed the rest of experiments with the support of C.B.F., A.R.E., E.F.H., M.A.H., and A.F. The gene expression analyses were supervised by A.G. and analyzed by H.F., M.G.Á. and I.C. designed the study and drafted the manuscript. I.C. and A.P. revised and edited the manuscript. All authors reviewed the results and approved the final manuscript.

## Data Availability Statement

The data that support the findings of this study are openly available in [PubMed] at [10.1093/bioline/iox039; 10.1073/pnas.2208040119], reference number [36279452].

## Keywords

bioengineering, endometrium, extracellular matrix hydrogel, organoids

Received: November 7, 2023  
Published online:

- [1] J. J. Brosens, M. S. Salker, G. Teklenburg, J. Nautiyal, S. Salter, E. S. Lucas, J. H. Steel, M. Christian, Y.-W. Chan, C. M. Boomsma, J. D. Moore, G. M. Hartshorne, S. Sucurovic, B. Mulac-Jericevic, C. J. Heijnen, S. Quenby, M. J. G. Koerkamp, F. C. P. Holstege, A. Shmygol, N. S. Macklon, *Sci. Rep.* **2014**, *4*, 3894.
- [2] B. Gellersen, I. Brosens, J. Brosens, *Semin. Reprod. Med.* **2007**, *25*, 445.
- [3] S. López-Martínez, A. Rodríguez-Eguren, L. De Miguel-Gómez, E. Francés-Herrero, A. Faus, A. Díaz, A. Pellicer, H. Ferrero, I. Cervelló, *Acta Biomater.* **2021**, *135*, 113.
- [4] A. Rodríguez-Eguren, L. De Miguel-Gómez, E. Francés-Herrero, M. Gómez-Álvarez, A. Faus, M. Gómez-Cerdá, I. Moret-Tatay, A. Díaz, A. Pellicer, I. Cervelló, *Hum. Reprod. Open* **2022**, *2023*, hoac053.
- [5] F. Liu, S. Hu, H. Yang, Z. Li, K. Huang, T. Su, S. Wang, K. Cheng, *Adv. Healthcare Mater.* **2019**, *8*, 1900411.
- [6] M. Y. Turco, L. Gardner, J. Hughes, T. Cindrova-Davies, M. J. Gomez, L. Farrell, M. Hollinshead, S. G. E. Marsh, J. J. Brosens, H. O. Critchley, B. D. Simons, M. Hemberger, B.-K. Koo, A. Moffett, G. J. Burton, *Nat. Cell Biol.* **2017**, *19*, 568.
- [7] Z. Zhao, X. Chen, A. M. Dowbaj, A. Sljukic, K. Bratlie, L. Lin, E. L. S. Fong, G. M. Balachander, Z. Chen, A. Soragni, M. Huch, Y. A. Zeng, Q. Wang, H. Yu, *Nat. Rev. Methods Primers*, **8**, 1900411.
- [8] C. Corró, L. Novellasdemunt, V. S. W. Li, *Am. J. Physiol. Cell Physiol.* **2020**, *319*, C151.
- [9] A. Luddi, V. Pavone, B. Semplici, L. Governini, M. Criscuoli, E. Paccagnini, M. Gentile, G. Morgante, V. De Leo, G. Belmonte, N. Zarovni, P. Piomboni, *Cells* **2020**, *9*, 1121.
- [10] E. Francés-Herrero, R. Lopez, M. Hellström, L. De Miguel-Gómez, S. Herraiz, M. Brännström, A. Pellicer, I. Cervelló, *Hum. Reprod. Update* **2022**, *28*, 798.
- [11] H. Poudel, K. Sanford, P. K. Szewo, R. Pathak, A. Ghosh, *ACS Omega* **2022**, *7*, 38.
- [12] C. Ma, K. Liu, Q. Li, Y. Xiong, C. Xu, W. Zhang, C. Ruan, X. Li, X. Lei, *Bioengineering (Basel, Switzerland)*. **2022**, *9*, 53.
- [13] S. A. Yi, Y. Zhang, C. Rathnam, T. Pongkulapa, K.-B. Lee, *Adv. Mater.* **2021**, *33*, 2007949.
- [14] M. J. Kratochvil, A. J. Seymour, T. L. Li, S. P. Pasca, C. J. Kuo, S. C. Heilshorn, *Nat. Rev. Mater.* **2019**, *4*, 606.
- [15] B. J. Klotz, L. A. Oosterhoff, L. Utomo, K. S. Lim, Q. Vallmajo-Martin, H. Clevers, T. B. F. Woodfield, A. J. W. P. Rosenberg, J. Malda, M. Ehrbar, B. Spee, D. Gawlitza, *Adv. Healthcare Mater.* **2019**, *8*, 1900979.
- [16] H.-J. Lee, M. J. Son, J. Ahn, S. J. Oh, M. Lee, A. Kim, Y.-J. Jeung, H.-G. Kim, M. Won, J. H. Lim, N.-S. Kim, C.-R. Jung, K.-S. Chung, *Acta Biomater.* **2017**, *64*, 67.
- [17] M. T. Kozlowski, C. J. Crook, H. T. Ku, *Commun. Biol.* **2021**, *4*, 1387.
- [18] Z. Gan, X. Qin, H. Liu, J. Liu, J. Qin, *Bioact. Mater.* **2023**, *28*, 386.
- [19] C. Gazia, R. Tamburrini, A. Asthana, D. Chaimov, S. M. Muir, D. I. Marino, L. Delbono, V. Villani, L. Perin, P. Di Nardo, J. Robertson, G. Orlando, *Curr. Opin. Organ Transplant.* **2019**, *24*, 604.
- [20] M. H. Cai, X. Y. Chen, L. Q. Fu, W. L. Du, X. Yang, X. Z. Mou, P. Y. Hu, *Front. Bioeng. Biotechnol.* **2021**, *9*, 630943.
- [21] A. D. Roth, P. Lama, S. Dunn, S. Hong, M.-Y. Lee, *Mater. Sci. Eng., C* **2018**, *90*, 634.
- [22] C. R. Taufer, M. A. Rodrigues-Da-Silva, G. W. Calloni, *Int. J. Dev. Biol.* **2020**, *64*, 433.
- [23] A. O. Abu-Yousif, I. Rizvi, C. L. Evans, J. P. Celli, T. Hasan, *J. Vis. Exp.* **2009**, *34*, e1692.
- [24] S. J. Winter, H. A. Miller, J. M. Steinbach-Rankins, *Pharmaceutics* **2021**, *13*, 1891.
- [25] S. Wang, D. Nagrath, P. C. Chen, F. Berthiaume, M. L. Yarmush, *Tissue Eng. Part A* **2008**, *14*, 227.
- [26] S. Sankar, K. O'Neill, M. Bagot D'arc, F. Rebeca, M. Buffer, E. Aleks, M. Fan, N. Matsuda, E. S. Gil, L. Spirio, *Front. Bioeng. Biotechnol.* **2021**, *9*, 679525.
- [27] 3-D Matrix Europe SAS, PuraSinus® Absorbable Haemostatic Material Instructions for Use, 2019. Retrieved from: [https://3dmatrix.com/wp-content/uploads/2020/05/PuraSinus\\_IFU\\_04\\_08\\_2020.pdf](https://3dmatrix.com/wp-content/uploads/2020/05/PuraSinus_IFU_04_08_2020.pdf) (accessed: June 2023).
- [28] M. F. B. Jamaluddin, A. Ghosh, A. Ingle, R. Mohammed, A. Ali, M. Bahrami, G. Kaiko, Z. Gibb, E. C. Filipe, T. R. Cox, A. Boulton, R. O'Sullivan, Y. Ius, A. Karakoti, A. Vinu, P. Nahar, K. Jaaback, V. Bansal, P. S. Tanwar, *Proc. Natl. Acad. Sci. USA* **2022**, *119*, e2208040119.
- [29] N. K. Karamanos, A. D. Theocharis, Z. Piperigkou, D. Manou, A. Passi, S. S. Skandalis, D. H. Vynios, V. Orian-Rousseau, S. Ricard-Blum, C. E. H. Schmelzer, L. Duca, M. Durbeek, N. A. Afratis, L. Troeberg, M. Franchi, V. Masola, M. Onisto, *FEBS J.* **2021**, *288*, 6850.
- [30] L. T. Saldin, M. C. Cramer, S. S. Velankar, L. J. White, S. F. Badylak, *Acta Biomater.* **2017**, *49*, 1.
- [31] P. M. Crapo, T. W. Gilbert, S. F. Badylak, *Biomaterials* **2011**, *32*, 3233.
- [32] B. N. Brown, S. F. Badylak, *Transl. Res.* **2014**, *163*, 268.
- [33] S. Bashir, M. Hina, J. Iqbal, A. H. Rajpar, M. A. Mujtaba, N. A. Alghamdi, S. Wageh, K. Ramesh, S. Ramesh, *Polymers* **2020**, *12*, 2702.
- [34] Y. Park, K. M. Huh, S. W. Kang, *Int. J. Mol. Sci.* **2021**, *22*, 2491.
- [35] S. López-Martínez, H. Campo, L. de Miguel-Gómez, A. Faus, A. T. Navarro, A. Díaz, A. Pellicer, H. Ferrero, I. Cervelló, *Front. Bioeng. Biotechnol.* **2021**, *9*, 639688.
- [36] J. Ahn, T. Sen, D. Lee, H. Kim, J. Y. Lee, H. S. Koo, J. J. Y. Kim, J. Y. Kim, J. Jang, Y. J. Kang, D. W. Cho, *Adv. Funct. Mater.* **2023**, *33*, 2214291.
- [37] H. Campo, X. García-Domínguez, S. López-Martínez, A. Faus, J. S. Vicente Antón, F. Marco-Jiménez, I. Cervelló, *Acta Biomater.* **2019**, *89*, 126.
- [38] S. A. Olalekan, J. E. Burdette, S. Getsios, T. K. Woodruff, J. J. Kim, *Biol. Reprod.* **2017**, *96*, 971.
- [39] E. Francés-Herrero, E. Juárez-Barber, H. Campo, S. López-Martínez, L. De Miguel-Gómez, A. Faus, A. Pellicer, H. Ferrero, I. Cervelló, *J. Pers. Med.* **2021**, *11*, 504.
- [40] Y. W. Chiu, W. P. Chen, C. C. Su, Y. C. Lee, P. H. Hsieh, Y. L. Ho, *Nanomed. Nanotechnol. Biol. Med.* **2014**, *10*, e1065.
- [41] M. A. Lancaster, M. Renner, C. A. Martin, D. Wenzel, L. S. Bicknell, M. E. Hurler, T. Homfray, J. M. Penninger, A. P. Jackson, J. A. Knoblich, *Nature* **2013**, *501*, 373.
- [42] K. H. Vining, D. J. Mooney, *Nat. Rev. Mol. Cell Biol.* **2017**, *18*, 728.
- [43] R. O. Hynes, A. Naba, *Cold Spring Harb. Perspect. Biol.* **2012**, *4*, a004903.
- [44] B. Sun, *Cell Rep* **2021**, *2*, 100515.
- [45] L. Albacete-Albacete, I. Navarro-Lérida, J. A. López, I. Martín-Padura, A. M. Astudillo, A. Ferrarini, M. Van-Der-Heyden, J. Balsinde, G. Orend, J. Vázquez, M. Á. del Pozo, *J. Cell Biol.* **2020**, *219*, e202006178.
- [46] T. Garrido-Gómez, F. Dominguez, A. Quiñero, C. Estella, F. Vilella, A. Pellicer, C. Simon, *FASEB J.* **2012**, *26*, 3715.

- [47] T. Tanaka, C. Wang, N. Umesaki, *Int. J. Mol. Med.* **2009**, *23*, 173.
- [48] S. Zeng, S. E. Ulbrich, S. Bauersachs, *BMC Genomics* **2019**, *20*, 895.
- [49] N. Salleh, N. Giribabu, *Sci. World J.* **2014**, *2014*, 201514.
- [50] A. Alok, A. A. Karande, *J. Reprod. Immunol.* **2009**, *83*, 124.
- [51] O. Mäentausta, R. Sormunen, V. Isomaa, V. Lehto, P. Jouppila, R. Vihko, *Lab Invest* **1991**, *65*, 582.
- [52] M. Saegusa, M. Hashimura, E. Suzuki, T. Yoshida, T. Kuwata, *Am. J. Pathol.* **2012**, *181*, 684.
- [53] K. Furuyama, Y. Kawaguchi, H. Akiyama, M. Horiguchi, S. Kodama, T. Kuhara, S. Hosokawa, A. Elbahrawy, T. Soeda, M. Koizumi, T. Masui, M. Kawaguchi, K. Takaori, R. Doi, E. Nishi, R. Kakinoki, J. M. Deng, R. R. Behringer, T. Nakamura, S. Uemoto, *Nat. Genet.* **2011**, *43*, 34.
- [54] Charles Rivers Laboratories, C57BL/6 Mouse Clinical Pathology Data. Retrieved from: [https://www.criver.com/sites/default/files/resources/doc\\_a/C57BL6MouseClinicalPathologyData.pdf](https://www.criver.com/sites/default/files/resources/doc_a/C57BL6MouseClinicalPathologyData.pdf).
- [55] A. M. Krensky, Y.-T. Ahn, *Nat. Clin. Pract. Nephrol.* **2007**, *3*, 164.
- [56] A. Bajwa, G. Kinsey, M. Okusa, *Curr. Drug Targets* **2009**, *10*, 1196.
- [57] E. Y. Jeon, L. Sorrells, H. E. Abaci, *Front. Bioeng. Biotechnol.* **2022**, *10*, 1038277.
- [58] R. Dong, S. Ma, X. Zhao, B. Wang, M. Roy, L. Yao, T. Xia, Y. Liu, *Front. Bioeng. Biotechnol.* **2022**, *10*, 1013217.
- [59] D. K. Baby, in *Rheology of Polymer Blends and Nanocomposites: Theory, Modeling and Applications* (Eds. S. Thomas, C. Sarathchandran, N. Chandran), Elsevier, Amsterdam, Netherlands, **2020**.
- [60] A. J. Engler, S. Sen, H. L. Sweeney, D. E. Discher, *Cell* **2006**, *126*, 677.
- [61] V. A. Schulte, K. Hahn, A. Dhanasingh, K.-H. Heffels, J. Groll, *Biofabrication* **2014**, *6*, 24106.
- [62] R. O. Hynes, *Science* **2009**, *326*, 1216.
- [63] National Center for Biotechnology Information (NCBI), LAMC2 laminin subunit gamma 2 [Homo sapiens (human)] – Gene – NCBI, <https://www.ncbi.nlm.nih.gov/gene/3918> (accessed August 2023).
- [64] FBN1 fibrillin 1 [Homo sapiens (human)] – Gene – NCBI, <https://www.ncbi.nlm.nih.gov/gene/2200>.
- [65] National Center for Biotechnology Information (NCBI), ANXA2 annexin A2 [Homo sapiens (human)] – Gene – NCBI, <https://www.ncbi.nlm.nih.gov/gene/302> (accessed August 2023).
- [66] H. Zhang, D. Xu, Y. Li, J. Lan, Y. Zhu, J. Cao, M. Hu, J. Yuan, H. Jin, G. Li, D. Liu, *Int. J. Biol. Sci.* **2022**, *18*, 2627.
- [67] E. Juárez-barber, E. Francés-herrero, A. Corachán, C. Vidal, J. Giles, P. Alamá, A. Faus, A. Pellicer, I. Cervelló, H. Ferrero, *J. Pers. Med.* **2022**, *12*, 219.
- [68] O. Chaudhuri, J. Cooper-White, P. A. Janmey, D. J. Mooney, V. B. Shenoy, *Nature* **2020**, *584*, 535.
- [69] S. Park, H. Yuk, R. Zhao, Y. S. Yim, E. W. Woldegebriel, J. Kang, A. Canales, Y. Fink, G. B. Choi, X. Zhao, P. Anikeeva, *Nat Commun* **2021**, *12*, 3435.
- [70] D.-M. Dai, D. Wang, D. Hu, W.-L. Wan, Y. Su, J.-L. Yang, Y.-P. Wang, F. Wang, L. Yang, H.-M. Sun, Y.-Y. Chen, X. Fang, J. Cao, J. Luo, K. Tang, R. Hu, H.-N. Duan, M. Li, W.-B. Xu, *Arch. Med. Sci.* **2020**, *16*, 522.
- [71] A. King, S. Balaji, L. D. Le, T. M. Crombleholme, S. G. Keswani, *Adv. Wound Care* **2014**, *3*, 315.
- [72] Z. Fan, M. Kong, W. Dong, C. Dong, X. Miao, Y. Guo, X. Liu, S. Miao, L. Li, T. Chen, Y. Qu, F. Yu, Y. Duan, Y. Lu, X. Zou, *Cell Death Dis.* **2022**, *13*, 495.
- [73] C. A. Dinarello, *Immunol. Rev.* **2018**, *281*, 8.
- [74] H. Campo, P. M. Baptista, N. López-Pérez, A. Faus, I. Cervelló, C. Simón, *Biol. Reprod.* **2017**, *96*, 34.
- [75] R. M. Ransohoff, M. Tani, *Trends Neurosci.* **1998**, *21*, 154.
- [76] M. N. Ajuebor, C. M. Hogaboam, S. L. Kunkel, A. E. I. Proudfoot, J. L. Wallace, *J. Immunol.* **2001**, *166*, 552.
- [77] A. E. I. Proudfoot, *Nat. Rev. Immunol.* **2002**, *2*, 106.
- [78] L. An, G.-Q. Dong, Q. Gao, Y. Zhang, L.-W. Hu, J.-H. Li, Y. Liu, *Photodermatol. Photoimmunol. Photomed.* **2010**, *26*, 28.
- [79] J.-H. Shi, H. Guan, S. Shi, W.-X. Cai, X.-Z. Bai, X.-L. Hu, X.-B. Fang, J.-Q. Liu, K. Tao, X.-X. Zhu, C.-W. Tang, D.-H. Hu, *Arch. Dermatol. Res.* **2013**, *305*, 341.
- [80] W. R. Proctor, M. Chakraborty, L. S. Chea, J. C. Morrison, J. D. Berkson, K. Semple, M. Bourdi, L. R. Pohl, *Hepatology* **2013**, *57*, 2026.